Journal of chemical & engineering data

Article

Cite This: J. Chem. Eng. Data XXXX, XXX, XXX−XXX

pubs.acs.org/jced

New Correlations for Prediction of High-Pressure Phase Equilibria of *n*-Alkane Mixtures with the RKPR EoS: Back from the Use of l_{ij} (Repulsive) Interaction Parameters

Natalia Giselle Tassin,[†] Sabrina Belén Rodríguez Reartes,[‡,§] and Martín Cismondi*,[†,∥]

[†]Instituto de Investigación y Desarrollo en Ingeniería de Procesos y Química Aplicada (IPQA), Universidad Nacional de Córdoba (UNC)-CONICET, X5016GCA Córdoba, Argentina

[‡]Planta Piloto de Ingeniería Química (PLAPIQUI), Universidad Nacional del Sur (UNS)-CONICET, 8000B Bahía Blanca, Buenos Aires, Argentina

[§]Departamento de Ingeniería Química, Universidad Nacional del Sur (UNS), 8000FTN Bahía Blanca, Buenos Aires, Argentina

[∥]CONICET, YPF Tecnología S.A. (Y-TEC), 1923 Berisso, Buenos Aires, Argentina

Supporting Information

ABSTRACT: After detecting some inadequate predictions of volumetric properties and solid−liquid equilibria with the RKPR Equation of State coupled to previously correlated parameters (Cismondi Duarte, M.; et al. *Fluid Phase Equilib.* **2015**, *403*, 49−59), we analyzed the causes and concluded that the problems were related to the predominant role of the *lij* repulsive interaction parameter on those correlations. With the aim of proposing a model able to describe in a correct and consistent way the phase and volumetric behavior of the *n*-alkane−*n*-alkane binary mixtures, including the more asymmetric ones, here we made a turn back from our previous parameter correlations. Leaving behind the use of *lij* parameters, which combined with the arithmetic average combining rule transforms the quadratic into a linear mixing rule for the covolume, we developed in this work for PR and RKPR EoS new correlations of the *kij* attractive parameters with temperature dependence for the homologous series of binary mixtures formed by methane, ethane, propane, *n*-butane, or *n*-pentane with heavier normal alkanes, adopting zero values when both carbon numbers are equal to or higher than six. This also involved a new parametrization of pure *n*-alkanes for the RKPR EoS and new volume shift correlations for both models. The results show a very good predictive power for the phase behavior of *n*-alkane binary systems, with RKPR showing a much better performance than that of PR in the case of the more asymmetric systems, and a correct description of volumetric properties.

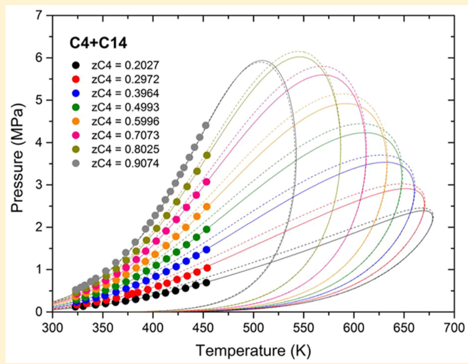

■ INTRODUCTION

The thermodynamic modeling of systems containing hydrocarbons under broad conditions of temperature, pressure, and composition is naturally of high interest for the oil industry. A correct and consistent description of the phase behavior for these types of multicomponent systems requires, first of all, a good representation of the behavior of the *n*-alkane−*n*-alkane constituent binaries. In particular, those systems presenting a high degree of asymmetry between their components and critical lines extending beyond 1000 bar at temperatures of interest for the oil industry (especially the methane binaries with heavier *n*-alkanes) cannot be reasonably represented with classic two-parameter Equations of State (EoS) like Soave−Redlich−Kwong (SRK)[2] or Peng−Robinson (PR)[3] with quadratic mixing rules. A review of different attempts to model these series of *n*-alkane mixtures, considering other types of models and approaches, was part of a preceding work.[1]

In previous studies[1,4] the superiority of the generalized Redlich−Kwong−Peng−Robinson Equation of State (RKPR EoS)[5] was demonstrated in comparison to the classic PR EoS[3] in the prediction of the vapor−liquid equilibrium (VLE) of the more asymmetric binary *n*-alkane−*n*-alkane mixtures and then also for multicomponent mixtures.[6] The present work was conceived as a continuation of those preceding studies and, at the same time, a turn back from the parameter correlations to which they arrived. The reason for such a turn back is the following. The correlations published in 2015[1] were meant to be the foundations for a more complete modeling of hydrocarbon mixtures that would consider different properties and other families of compounds beyond *n*-alkanes. For simplicity, we will term the obtained predictive models for *n*-alkane mixtures as RKPR2015 and PR2015. RKPR2015 predictions were excellent for fluid phase equilibria and clearly superior to those of the PR2015 EoS in the more asymmetric

Special Issue: Latin America

Received: November 7, 2018
Accepted: February 14, 2019

DOI: 10.1021/acs.jced.8b01050
J. Chem. Eng. Data XXXX, XXX, XXX−XXX

cases, not only for binary systems[1] but also for multicomponent fluids.[6] Nevertheless, we then discovered serious limitations in the prediction of mixture liquid densities or volumes and also in the modeling of solid−liquid saturation curves. We concluded that both problems were related, and the reason depended on the predominant role of the *lij* interaction parameter in the RKPR2015 correlations. This is illustrated in Figure 1. First, for the mixture volume of the methane + *n*-decane binary system at 100 °C (in the typical range of reservoir temperatures) and 1000 bar, RKPR2015 provided better predictions for the fluid phase equilibria, helped by a negative *lij* value, but its effect on the mixture covolume leads to an artificial curvature in the volume−composition curve, which does not agree with the experimental data presenting an almost linear behavior or probably small negative excess volumes, as predicted by PR2015 with a linear mixing rule for the covolume (see the zoomed-in region of the upper part of Figure 1). Then, at the bottom part of Figure 1, another consequence of the same covolume distortion: a wrong slope for the solid−liquid phase envelope is predicted for a mixture of methane + *n*-eicosane.

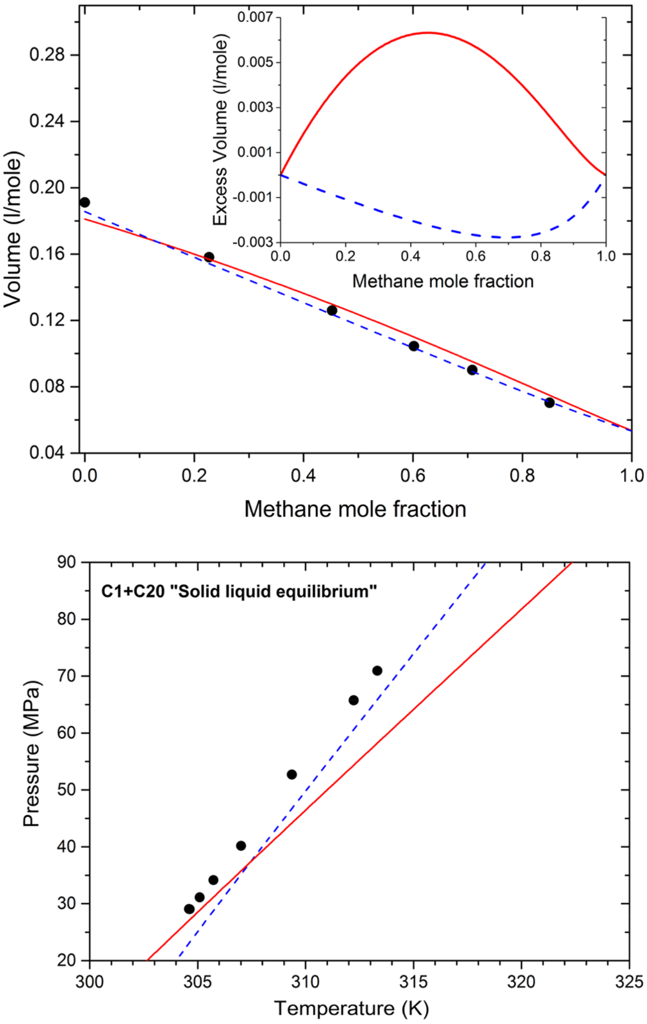

Figure 1. Illustration of two different types of pitfalls when making predictions based on RKPR2015. Upper: Mixture molar volume and excess volume for the system methane + *n*-decane at 373.15 K and 1000 bar. Dots: Experimental data from Regueira et al.[7] Bottom: Solid−liquid phase envelope for a mixture of methane + *n*-eicosane, with mole fractions of 0.637 and 0.363, respectively. Dots: Experimental data from ref 8. Calculations with the PR EoS (dashed lines) and RKPR2015 EoS (solid line) correspond to quadratic mixing rules with parameters from ref 1 and volume translations according to ref 6.

To overcome these problems, the development of new correlations of *kij* interaction parameters with temperature dependence for all possible pairs of normal alkanes is the focus of this work (for PR and RKPR EoS), along with the use of a null *lij* interaction parameter, i.e., a linear mixing rule for the covolume. This also required a new parametrization of pure *n*-alkanes for the RKPR EoS.

■ METHODOLOGY AND PARAMETRIZATION STRATEGY

Experimental Data Selected and Objective Function. As this work aims at developing new parameter correlations that do not suffer from the problems found for those correlations proposed in previous works,[1,4] the experimental information used in those works has been considered in the present study. However, the database used here is larger, since in addition to the series of methane, ethane, and propane, the series of butane + *n*-alkanes was incorporated in order to be able to correlate the corresponding parameters. The experimental information looked at here came from more than 70 publications ranging from the years 1934 to 2012.

It is important to clarify that to simplify the notation of *n*-alkanes, hereafter we will refer equally to C4 or *n*-C4 for the case of *n*-butane for example.

For optimizing the methane + *n*-alkane series (the most challenging series to correlate and which contains the most asymmetric systems), 12 binary systems were considered spanning the carbon number range from ethane (C2) to *n*-hexatriacontane (C36). A total of 131 experimental data were adjusted, including critical points, biphasic points (with compositional information for both phases), bubble points, and dew points. For the ethane series, a total of 9 systems were selected from *n*-butane (C4) to *n*-hexatriacontane (C36), and 94 experimental points of the same type as the methane series were fitted. The propane series covers a total of 13 binary systems that correspond to the extended range of *n*-butane (C4) to *n*-hexacontane (C60), adjusting 84 experimental data. The new series incorporated in this work, the *n*-butane series, covers 3 systems from *n*-decane (C10) to *n*-hexacontane (C60), and 23 experimental points were adjusted.

Table 1 summarizes the type and number of points selected for each system, together with the temperature and pressure ranges covered. The specific information and corresponding references can be found in Section A of the Supporting Information in Tables S1−S15. The number of "P_{sat}" points for the specified temperature and composition considers both bubble and dew points. For example, the number 6 indicated for system C_1 + C_3 is the result of three bubble points (Table S9 in Section A of the Supporting Information) plus three dew points (Table S13 in Section A of the Supporting Information).

The parametrization strategy and methodology were essentially the same as in our previous works.[1,4] The generalized objective function used for developing general correlations for the different series of binary systems is given in eq 1, where KP_i is either the temperature or the pressure coordinate of a binary phase equilibrium key point. The

DOI: 10.1021/acs.jced.8b01050
J. Chem. Eng. Data XXXX, XXX, XXX−XXX

Table 1. Type and Number of Experimental Points (and Covered $T-P$ Ranges) Considered for the Optimization of the Interaction Parameters for Methane, Ethane, Propane, and n-Butane + n-Alkane Systems with the PR and RKPR EoS

system	critical	$x-y$ ($T-P$)	P_{sat} (T, z)	T range (K)	P range (bar)
$C_1 + C_2$	2	5	0	210.0−270.0	16.1−66.5
$C_1 + C_3$	2	8	6	144.3−344.3	2.1−84.1
$C_1 + C_4$	2	4	4	222.1−377.6	6.9−126.2
$C_1 + C_5$	2	6	6	176.2−273.2	20.7−151.2
$C_1 + C_6$	2	6	3	198.1−423.0	27.6−201.6
$C_1 + C_{10}$	2	3	5	277.6−583.1	27.2−361.3
$C_1 + C_{14}$	2	0	8	294.0−447.6	20.7−540.0
$C_1 + C_{16}$	2	0	8	292.7−350.0	45.3−695.5
$C_1 + C_{20}$	2	2	5	305.8−573.2	20.1−890.0
$C_1 + C_{24}$	2	0	8	322.6−453.2	119.2−1047.0
$C_1 + C_{30}$	2	0	8	341.2−472.5	66.0−1142.0
$C_1 + C_{36}$	2	3	9	373.0−573.0	20.0−1274.0
$C_2 + C_4$	2	7	4	303.2−394.3	17.3−58.1
$C_2 + C_5$	2	6	4	277.6−410.9	10.3−68.3
$C_2 + C_{10}$	2	6	5	277.6−510.9	6.9−103.4
$C_2 + C_{16}$	2	0	7	302.7−453.0	24.9−138.0
$C_2 + C_{20}$	2	0	8	310.7−451.5	16.5−160.5
$C_2 + C_{22}$	0	0	11	300.0−360.0	13.5−92.8
$C_2 + C_{24}$	2	0	7	310.0−360.0	11.5−144.0
$C_2 + C_{28}$	2	1	6	330.0−360.0	17.6−164.8
$C_2 + C_{36}$	2	0	6	350.0−573.2	13.6−224.0
$C_3 + C_4$	2	5	1	273.2−410.9	1.4−44.0
$C_3 + C_6$	2	0	5	383.2−497.0	10.3−49.9
$C_3 + C_8$	2	0	4	359.9−524.2	24.1−59.6
$C_3 + C_{10}$	2	4	3	323.4−477.6	6.9−70.9
$C_3 + C_{14}$	2	0	2	378.0−408.0	33.6−65.0
$C_3 + C_{20}$	0	0	7	309.1−358.6	5.2−32.5
$C_3 + C_{32}$	2	0	5	378.2−408.2	48.8−92.3
$C_3 + C_{34}$	2	0	8	336.7−428.2	10.5−110.0
$C_3 + C_{36}$	2	0	6	378.2−408.2	50.7−100.5
$C_3 + C_{40}$	2	0	5	363.0−431.0	37.8−116.7
$C_3 + C_{46}$	2	0	2	378.2−408.2	63.1−115.8
$C_3 + C_{54}$	2	0	1	378.2−408.2	93.2−134.7
$C_3 + C_{60}$	2	0	6	378.2−429.0	18.4−141.8
$C_4 + C_{10}$	2	4	1	377.6−518.9	10.3−49.0
$C_4 + C_{14}$	0	0	6	403.0−453.0	8.4−44.0
$C_4 + C_{60}$	2	4	4	433.2−453.2	58.0−87.2

superscript "exp" means "experimental value", while the superscript "calc" means "calculated value".

$$\mathrm{OF} = \sum_{i=1}^{\mathrm{NTP}} \frac{(\mathrm{KP}_i^{\mathrm{calc}} - \mathrm{KP}_i^{\mathrm{exp}})^2}{\mathrm{KP}_i^{\mathrm{exp}}} + \sum_{j=1}^{\mathrm{NZ}} \left[\left| \ln\left(\frac{z_{j,1}^{\mathrm{calc}}}{z_{j,1}^{\mathrm{exp}}}\right) \right| + \left| \ln\left(\frac{z_{j,2}^{\mathrm{calc}}}{z_{j,2}^{\mathrm{exp}}}\right) \right| \right] \tag{1}$$

In this work, as in the previous ones, KP_i can be a binary mixture critical pressure (P_c) (Tables S1 to S4 in Section A of the Supporting Information) at a specified temperature or a saturation pressure at given temperature and composition (Tables S9 to S15 in Section A of the Supporting Information); z_{j1} and z_{j2} are, respectively, the mole fractions of the light n-alkane (1) (i.e., methane, ethane, propane, or n-butane) and of the heavier n-alkane (2). These mole fractions can be the critical composition (Tables S1 to S4 in Section A of the Supporting Information) or the composition of a phase under two-phase equilibrium conditions at given temperature and pressure (Tables S5 to S8 in Section A of the Supporting Information). NTP is the number of experimental pressure and temperature values used in the objective function. Analogously, NZ is the number of experimental mole fraction vectors used in the objective function. Note that the terms for temperature and pressure coordinates are not dimensionless and that the values should be in K and bar, respectively.

Cubic Equations of State with Two and Three Parameters: PR and RKPR EoS. In this work, we developed new correlations for prediction of high-pressure phase equilibria of n-alkane mixtures with the PR and RKPR EoS. Although the use of two- and three-parameter cubic Equations of State to describe the phase behavior of asymmetric mixtures has been previously discussed,[1,4] the purpose of this subsection is to provide a summary of these types of equations and their main differences, in particular, those used in this work: Peng−Robinson Equation of State[3] (PR EoS) with two parameters and generalized Redlich−Kwong−Peng−Robinson[5] (RKPR EoS) with three parameters. Møllerup and Michelsen[9] proposed the following general expression, shown in eq 2, in which all of the well-known cubic EoS are contained for particular pairs of values (δ_1, δ_2)

$$P = \frac{RT}{v - b} - \frac{a(T)}{(v + \delta_1 b)(v + \delta_2 b)} \tag{2}$$

When the delta constants are $(1 + \sqrt{2};\ 1 - \sqrt{2})$, the PR equation is obtained, as (0, 0) leads to the vdW, and (1,0) leads to the RK. Then, if we add the following restriction

$$-\delta_1\delta_2 = \delta_1 + \delta_2 - 1 = c \tag{3}$$

and transform the constant δ_1 into a compound-specific parameter, we have a three-parameter Equation of State, which connects the RK ($c = 0$) and PR ($c = 1$) density dependences with the following expressions for the compressibility factor (eqs 4−6)

$$z_{\mathrm{RKPR}} = \frac{1}{1 - 4\eta} - \frac{4\eta\tau}{(1 + 4\delta_1\eta)\left(1 + 4\frac{1-\delta_1}{1+\delta_1}\eta\right)} \tag{4}$$

$$\tau = \frac{a}{RTb} \tag{5}$$

$$\eta = \frac{b}{4v} \tag{6}$$

As it has been widely studied and discussed previously,[5,4,1] the intrinsic limitations of two-parameter cubic Equations of State to reproduce volumetric and derived properties in some cases, rather than their empirical character, come from the fact that every two-parameter Equation of State for which the compressibility factor can be expressed in terms of two dimensionless variables that are directly or inversely proportional to the molar volume and/or the temperature is a corresponding states model. This was demonstrated by Møllerup,[9] and the details of this demonstration can be consulted in appendix A of the original work of the RKPR EoS.[5]

In order to overcome the limitations of a two-parameter cubic Equation of State, a third compound-specific parameter in the density of the Equation of State is necessary to model different types of fluids and their asymmetric mixtures. In the case of RKPR EoS, this third parameter is δ_1, a structural parameter, which increases with nonsphericity (and also with polarity, but polarity is not present in alkanes). This parameter

DOI: 10.1021/acs.jced.8b01050
J. Chem. Eng. Data XXXX, XXX, XXX−XXX

comes from eq 11 in the "Pure Compound Parameters" section of this article.

The expressions for the residual Helmholtz energy and pressure in the RKPR EoS are the following (eqs 7−9)

$$\frac{A^{\mathrm{res}}}{RT} = -\ln\left(1 - \frac{b}{v}\right) - \frac{a}{RTb\left(\delta_1 - \frac{1-\delta_1}{1+\delta_1}\right)}\ln\left(\frac{v + \delta_1 b}{v + \frac{1-\delta_1}{1+\delta_1}b}\right) \tag{7}$$

$$a = a_c\left(\frac{3}{2 + T_r}\right)^k \tag{8}$$

$$P = \frac{RT}{v - b} - \frac{a_c\left(\frac{3}{2+T_r}\right)^k}{(v + \delta_1 b)\left(v + \frac{1-\delta_1}{1+\delta_1}b\right)} \tag{9}$$

Further details of the deduction of these expressions can be found in the original reference of the RKPR EoS.[5]

As it is well-known, a temperature dependence for the attractive parameter a is required to achieve a reasonable quantitative agreement with experimental data, especially for vapor pressures. Instead of Soave's[2] classic α function, which with different coefficients is also used in the PR EoS[3] and is known to lead to different types of inconsistencies, in the RKPR EoS, another α function is used

$$\alpha = \frac{a}{a_c} = \left(\frac{3}{2 + T_r}\right)^k \tag{10}$$

This function is finite, positive, and monotonically decreases from a finite value at 0 K toward zero at infinite temperature. This condition of the α function has been studied by Yang et al.,[10] where modifications to the Soave function are proposed in order to avoid physical inconsistencies in the supercritical region. The α function proposed by Yang et al.[10] satisfies the same requirements as the one in the RKPR EoS.

Adopting the two classical restrictions (T_c and P_c) for the determination of the three parameters at the critical point, having decided that δ_1 as well as b will be constant for each fluid and also adopted a standard procedure to determine the temperature dependence of a, the RKPR EoS provides one extra degree of freedom in comparison to a classic two-parameter cubic EOS like SRK or PR, and different approaches were followed in previous articles. In the original RKPR development, Cismondi and Mollerup[5] proposed the relation $Z_c^{\mathrm{EOS}} = 1.168 Z_c^{\mathrm{exp}}$ as the default setting for nonassociating fluids, which was later followed by other authors.[11−13] In other works, Cismondi et al. decided to impose the reproduction of the liquid density at a specified temperature, either at the triple point[14] or at $T_r = 0.70$.[15]

In recent works, it was found that predictions of phase equilibria for asymmetric mixtures were quite sensitive to the values of δ_1, and therefore, it was proposed that this third parameter of the RKPR model could be defined based not only on properties of pure compounds but also on the basis of properties of binary systems, particularly of the most difficult series to model among hydrocarbon mixtures: the asymmetric series of methane + n-alkanes; it was first performed for individual systems[4] and then for the entire homologous series.[1] In summary, the approach adopted here was that the parameters of pure compounds come from reproducing T_c, P_c, and ω and imposing a value of δ_1.

Pure Compound Parameters. As previously stated, in this work, the Peng−Robinson EoS was implemented in the original and traditional way, i.e., the a_c and b parameters for each fluid were calculated from T_c and P_c, while the constant m for the temperature dependence of a was calculated from the acentric factor (ω). In the case of the RKPR EoS, besides also allowing for the exact reproduction of the experimental T_c and P_c for each fluid and matching the acentric factor based on adjusting the constant k (which defines the attractive parameter temperature dependence, see eq 10), the model provides one extra degree of freedom, namely, the third parameter δ_1, in comparison to a classic two-parameter cubic EoS like SRK or PR.[5] For the RKPR EoS, it is important to point out that the results in this work correspond to a redesign of the δ_1 curve for n-alkanes, which was performed together with the optimization of interactions for the methane series. The justification for this nonclassic approach has been provided elsewhere.[4] The functionality chosen for the δ_1 parameter is shown in eq 2, where CN is the n-alkane carbon number; A_d, B_d, and refN are the parameters associated with the δ_1 correlation.

$$\delta_1 = A_d + B_d(1 - \mathrm{e}^{-(\mathrm{CN}/\mathrm{refN})}) \tag{11}$$

The optimum values encountered for the parameters are A_d = 2.70, B_d = 0.4981, and refN = 30.437. The resulting evolution of this third parameter of the RKPR EoS in the normal alkane's family can be appreciated in Figure 2.

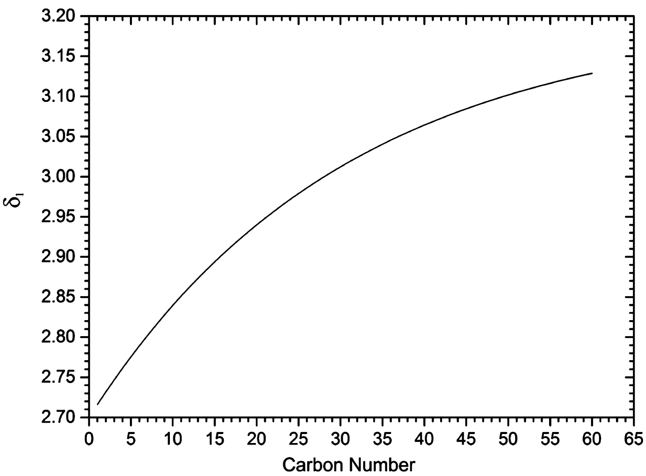

Figure 2. RKPR EoS third parameter (δ_1) values for n-alkanes with the new correlation (eq 11).

Table 2 provides the numerical values for all the parameters, obtained from matching the critical temperature and pressure, besides the acentric factor, for n-alkanes up to C60. The consideration of the critical constants for the heavier n-alkanes has been detailed in the previous work,[1] and the same criterion has been maintained. We adopted in essence the approach proposed by Schwarz and Nieuwoudt[16] to heavier n-alkanes and used the DIPPR values available until C36.

Mixing Rules and Temperature Dependence. Classic quadratic van der Waals mixing rules were used, considering only an attractive kij interaction parameter with temperature dependence according to eq 12, where T_{C1} is the critical temperature of the more volatile compound. Therefore, there

DOI: 10.1021/acs.jced.8b01050
J. Chem. Eng. Data XXXX, XXX, XXX−XXX

Table 2. Pure Compound Parameters for the RKPR EoS

ID	a_c (bar L^2/mol^2)	b (L/mol)	δ_1	k	T_c (K)	P_c (bar)	ω
C1	2.533	0.026	2.716	1.125	190.56	45.99	0.012
C2	6.144	0.039	2.732	1.491	305.32	48.72	0.099
C3	10.346	0.055	2.747	1.703	369.83	42.48	0.152
C4	15.309	0.070	2.761	1.890	425.12	37.96	0.200
C5	21.065	0.087	2.775	2.087	469.70	33.70	0.252
C6	27.425	0.105	2.789	2.273	507.60	30.25	0.301
C7	34.314	0.123	2.802	2.450	540.20	27.40	0.350
C8	41.874	0.143	2.815	2.630	568.70	24.90	0.400
C9	49.803	0.162	2.828	2.784	594.60	22.90	0.444
C10	58.366	0.183	2.839	2.953	617.70	21.10	0.492
C11	67.624	0.204	2.851	3.081	639.00	19.50	0.530
C12	76.869	0.225	2.862	3.235	658.00	18.20	0.576
C13	87.679	0.250	2.873	3.370	675.00	16.80	0.617
C14	98.943	0.275	2.884	3.451	693.00	15.70	0.643
C15	109.606	0.297	2.894	3.590	708.00	14.80	0.686
C16	120.888	0.321	2.904	3.687	723.00	14.00	0.717
C17	130.943	0.341	2.913	3.850	736.00	13.40	0.770
C18	142.384	0.365	2.922	3.977	747.00	12.70	0.811
C19	153.944	0.388	2.931	4.100	758.00	12.10	0.852
C20	164.913	0.410	2.940	4.262	768.00	11.60	0.907
C21	176.929	0.434	2.948	4.363	778.00	11.10	0.942
C22	189.659	0.459	2.956	4.449	787.00	10.60	0.972
C23	201.706	0.482	2.964	4.603	796.00	10.20	1.026
C24	214.257	0.506	2.972	4.728	804.00	9.80	1.071
C25	225.523	0.527	2.979	4.822	812.00	9.50	1.105
C26	239.593	0.555	2.986	4.955	819.00	9.10	1.154
C27	251.240	0.576	2.993	5.113	826.00	8.83	1.214
C28	264.884	0.603	3.000	5.175	832.00	8.50	1.238
C29	276.610	0.625	3.006	5.246	838.00	8.26	1.265
C30	289.790	0.649	3.012	5.353	844.00	8.00	1.307
C32	317.397	0.701	3.024	5.527	855.00	7.50	1.377
C34	342.225	0.746	3.035	5.669	864.80	7.12	1.432
C36	366.175	0.789	3.045	5.899	874.00	6.80	1.526
C38	395.163	0.842	3.055	6.005	882.00	6.42	1.571
C40	421.890	0.890	3.064	6.166	889.60	6.12	1.640
C42	449.283	0.940	3.073	6.326	896.60	5.84	1.710
C44	476.386	0.988	3.081	6.488	903.10	5.59	1.780
C46	503.740	1.037	3.088	6.641	909.20	5.36	1.849
C48	530.934	1.085	3.095	6.794	914.80	5.15	1.919
C50	558.856	1.135	3.102	6.943	920.00	4.95	1.989
C52	586.308	1.184	3.108	7.088	924.90	4.77	2.058
C54	614.205	1.233	3.114	7.232	929.50	4.60	2.128
C56	642.539	1.283	3.119	7.371	933.90	4.44	2.197
C58	669.313	1.330	3.124	7.516	937.90	4.30	2.267
C60	697.758	1.379	3.129	7.654	941.80	4.16	2.337

are two parameters that can be correlated for each homologue series: k_{ij}^{inf} and k'_{ij}, where "i" represents the most volatile compound, and "j" represents the least volatile compound.

$$k_{ij} = k_{ij}^{\text{inf}} + k'_{ij}e^{-(T/T_{C1})} \tag{12}$$

After different studies on the functionality of the parameters involved in the computation of the kij interaction parameter are performed, eqs 13 and 14 are proposed for the calculation of k'_{ij}, and k_{ij}^{inf}, respectively.

$$k'_{ij} = c_k\left(\frac{\text{CN} - \text{CN}^*}{\text{CN}}\right)^{e_k} + d_k(\text{CN} - \text{CN}^*)e^{-(2(\text{CN}-\text{CN}^*)/\text{refN})} \tag{13}$$

$$k_{ij}^{\text{inf}} = b_k(1 - e^{-(\text{CN}-\text{CN}^*/\text{refN})}) \tag{14}$$

where CN is the carbon number of the heavier compound, and CN* is the carbon number of the most volatile compound in the system considered, i.e., the one defining the series. c_k, b_k, d_k, e_k, and refN are the parameters that we correlate in this work in order to adjust the homologous series of methane, ethane, propane, and n-butane with n-alkanes. Tables 3 and 4 show the optimized values for the mentioned parameters for RKPR and PR EoS, respectively. For the methane series, eq 13 is applied starting at CN = 5, while for the previous three pairs, a null k'_{ij} is used.

It is important to note that the first four series were optimized on the basis of experimental data (Tables S1−S15 in the Section A of the Supporting Information), while the C_5 + n-alkanes series was estimated based on the trends observed in

DOI: 10.1021/acs.jced.8b01050
J. Chem. Eng. Data XXXX, XXX, XXX−XXX

Table 3. Optimized Constants for the Calculations of k'_{ij} and k_{ij}^{inf} Values for the Binary Series from C1 to C5 through Eqs 13 and 14 for the RKPR EoS

series	c_k	d_k	e_k	b_k	refN
methane	−0.2077	0.0608	0.3993	0.0387	30.4370
ethane	0.2631	−0.0150	1.7766	−0.0859	30.4370
propane	0.2462	−0.0109	1.5426	−0.1021	30.4370
n-butane	0.1891	−0.0079	1.6275	−0.0656	30.4370
n-pentane	0.1450	−0.0073	1.7000	−0.0430	30.4370

Table 4. Optimized Constants for the Calculations of k'_{ij} and k_{ij}^{inf} Values for the Binary Series from C1 to C5 through Eqs 13 and 14 for the PR EoS

series	c_k	d_k	e_k	b_k	refN
methane	−0.5199	0.0741	2.9520	0.1066	38.3685
ethane	−0.1630	0.0150	1.6600	0.0902	38.3685
propane	−0.1606	0.0167	1.4616	0.0881	38.3685
n-butane	−0.1590	0.0250	1.3502	0.0748	38.3685
n-pentane	−0.1480	0.0270	1.3800	0.0670	38.3685

the optimized parameters. The k'_{ij} and k_{ij}^{inf} interactions were considered null from the C_6 + n-alkanes series onward. Table 5 presents the interaction parameters obtained from the optimized correlations and the corresponding minimum values for the objective function for the series considered in this work.

Volume Shift. In order to improve molar volume predictions without affecting phase equilibrium calculations, a volume translation strategy was implemented for both models, following the guidelines originally proposed by Péneloux et al.[17] that were extended by Zabaloy and Brignole[18] and then by Jaubert et al.[19]

To evaluate the predictions against the experimental behavior, the multiparametric equations of Span and Wagner[20] were used as a reference for the most volatile n-alkanes up to n-octane. For the heavier n-alkanes, the works that appear in Table 6 were selected as the source of experimental data, since they provide volumetric information. In Table 6, the type (isothermic or isobaric) and the range of the experimental data are indicated.

For the RKPR EoS, the determinations of the volume translations were made by calculating the average of the differences between the experimental volumes and the volumes calculated with the RKPR at a few selected pressures for each available isotherm or for selected temperatures along each isobar. The experimental volumes considered correspond to the conditions and systems reported in Table 6. The values of such averages appear as dots (empty and filled) in Figure 3. It is clearly observed that the average differences for n-octane and lighter n-alkanes are low, compared to those of heavier alkanes. On this basis, two different correlations for the volume shift parameter were obtained by linear regression. The correlation of eq 15 was found for the n-alkanes from C1 to n-C8, while for the heavier n-alkanes (from n-C10 to n-C64), the correlation of eq 16 was obtained. In eqs 15 and 16, CN corresponds to the carbon number of the n-alkane. The coefficient of determination of eq 15 is 0.95035, whereas for eq 16, it is 0.98773. For the volume shift of n-C9, an average value between the volume shifts considered for n-C8 and n-C10 was calculated.

$$V_{\mathrm{shift-RKPR\,EoS}} = 2.068210^{-4}\mathrm{CN}^2 - 1.510510^{-3}\mathrm{CN} - 4.233110^{-3};\ \mathrm{CN} = 1\text{ to }8 \tag{15}$$

$$V_{\mathrm{shift-RKPR\,EoS}} = 9.166410^{-7}\mathrm{CN}^3 - 1.232410^{-4}\mathrm{CN}^2 + 9.652110^{-3}\mathrm{CN} - 7.8080610^{-2};\ \mathrm{CN} = 10\text{ to }64 \tag{16}$$

Figure 3 shows the correlated volume shifts obtained for the whole range of n-alkanes from C1 to n-C64 for the RKPR EoS. Small negative translations are obtained for the lighter n-alkanes, whereas larger positive corrections are obtained for heavier n-alkanes, reaching a value of 0.28 L/mol for n-C64.

In the case of the PR EoS, volume shift values for lighter n-alkanes from C1 to n-C6 were obtained as proposed by Pedersen et al.[28] (see empty dots in Figure 3). For heavier n-alkanes (from n-C8 to n-C64), the determinations of the volume translations were also made by calculating the average of the differences between the experimental volumes and the volumes calculated with the PR (filled dots in Figure 4). But for this EoS, apart from the experimental data and conditions considered for the RKPR (see Table 6), the experimental volume of the n-alkanes measured at 298.25 K and 1 atm of pressure was also considered (data from DIPPR[29]).

Thus, for the PR EoS, the volume shifts applied for the n-alkanes from C1 to n-C6 were those proposed by Pedersen et al.,[28] while for the heavier n-alkanes (from n-C8), the correlation of eq 17 was applied. In eq 17, CN corresponds to the carbon number of the n-alkane. The coefficient of determination of eq 17 is 0.99775. For n-C7, the volume shift parameter was obtained as an average value between the volume shifts accounted for n-C6 and n-C8.

$$V_{\mathrm{shift-PR\,EoS}} = 4.961110^{-6}\mathrm{CN}^3 - 3.634710^{-4}\mathrm{CN}^2 + 1.543810^{-2}\mathrm{CN} - 1.068010^{-1};\ \mathrm{CN} = 8.64 \tag{17}$$

Figure 4 shows the volume shifts obtained for the n-alkanes from C1 to n-C64 for the PR EoS. As in the case of RKPR EoS, for light n-alkanes, the corrections are small negative values, and the volume translations increase with the increment of carbon number. However, a higher maximum volume translation is obtained for the PR EoS compared to that of the RKPR EoS, reaching a value of almost 0.7 L/mol for n-C64.

It is worth noting that even though the correlations of eqs 15 and 16 are here defined by considering the carbon numbers of the n-alkanes, an extrapolation of these correlations to other alkanes (i.e., branched or cyclic alkanes) could be proposed by means of a "scale transformation" as proposed by Tassin et al.[6] In the work of by Tassin et al.,[6] we have implemented a simple approach to extend the correlations defined for normal alkanes (in terms of carbon numbers) to branched alkanes. In such an approach, an equivalent carbon number ($\mathrm{CN_{EQ}}$) equal to ω/0.05 (i.e., the acentric factor of the branched alkane divided by 0.05) is calculated and then used for the correlations previously defined for normal alkanes. The effect of that approach is a "scale transformation", from NC to ω. This kind of application is beyond the scope of the present work, but could be considered and probably applied with success as in our previous experience.

For mixtures of two or more components, as in the case of the parameters of each EoS, the volume translation parameter

DOI: 10.1021/acs.jced.8b01050
J. Chem. Eng. Data XXXX, XXX, XXX−XXX

Table 5. Interaction Parameters from the Optimized Correlations[a] and the Corresponding Minimum Values for the Objective Function for Methane, Ethane, Propane, and n-Butane with n-Alkanes Systems for Both PR and RKPR EoS

	RKPR EoS			PR EoS		
system	k'_{ij}	k^{inf}_{ij}	OF contribution	k'_{ij}	k^{inf}_{ij}	OF contribution
$C_1 + C_2$	0	0.00125	0.502	0	0.00274	0.485
$C_1 + C_3$	0	0.00246	2.118	0	0.00541	2.131
$C_1 + C_4$	0	0.00363	5.542	0	0.00802	5.263
$C_1 + C_5$	−0.00301	0.00477	13.844	−0.02844	0.01055	13.661
$C_1 + C_6$	0.02575	0.00586	8.680	−0.01802	0.01302	7.056
$C_1 + C_{10}$	0.10376	0.00991	6.727	0.03625	0.02229	2.888
$C_1 + C_{14}$	0.13476	0.01345	11.126	0.07143	0.03064	8.119
$C_1 + C_{16}$	0.13794	0.01506	29.258	0.07884	0.03449	32.722
$C_1 + C_{20}$	0.12798	0.01797	29.952	0.07609	0.04163	41.488
$C_1 + C_{24}$	0.10431	0.02052	21.284	0.05537	0.04806	55.803
$C_1 + C_{30}$	0.05735	0.02377	15.812	0.00354	0.05654	42.322
$C_1 + C_{36}$	0.00801	0.02645	25.622	−0.06005	0.06379	82.808
total OF for the methane + n-alkane series			**162.309**			**294.745**
$C_2 + C_4$	0.05049	−0.00546	0.993	−0.02455	0.00458	1.789
$C_2 + C_5$	0.06922	−0.00806	1.722	−0.03132	0.00678	1.822
$C_2 + C_{10}$	0.10605	−0.01985	2.901	−0.03346	0.01698	2.034
$C_2 + C_{16}$	0.12384	−0.03167	4.267	−0.02937	0.02758	1.722
$C_2 + C_{20}$	0.13545	−0.03835	3.347	−0.03119	0.03378	8.577
$C_2 + C_{22}$	0.14151	−0.04137	0.570	−0.03338	0.03664	7.293
$C_2 + C_{24}$	0.14767	−0.04421	1.728	−0.03625	0.03936	10.533
$C_2 + C_{28}$	0.16000	−0.04934	4.765	−0.04356	0.04440	20.940
$C_2 + C_{36}$	0.18308	−0.05779	6.037	−0.06157	0.05302	47.481
total OF for the ethane + n-alkane series			**26.329**			**102.192**
$C_3 + C_4$	0.01880	−0.00330	0.929	−0.00532	0.00227	1.076
$C_3 + C_6$	0.05766	−0.00958	0.136	−0.01546	0.00663	0.173
$C_3 + C_8$	0.08000	−0.01547	0.251	−0.01646	0.01076	0.245
$C_3 + C_{10}$	0.09385	−0.02098	7.268	−0.01419	0.01469	7.207
$C_3 + C_{14}$	0.11152	−0.03097	1.524	−0.00936	0.02196	1.475
$C_3 + C_{20}$	0.13097	−0.04369	0.054	−0.00961	0.03153	1.339
$C_3 + C_{32}$	0.16450	−0.06272	0.885	−0.03227	0.04673	3.197
$C_3 + C_{34}$	0.16943	−0.06523	1.874	−0.03744	0.04883	15.447
$C_3 + C_{36}$	0.17414	−0.06757	1.552	−0.04275	0.05082	4.839
$C_3 + C_{40}$	0.18284	−0.07182	1.866	−0.05350	0.05451	7.492
$C_3 + C_{46}$	0.19409	−0.07724	1.466	−0.06919	0.05938	4.910
$C_3 + C_{54}$	0.20594	−0.08299	2.158	−0.08806	0.06478	7.190
$C_3 + C_{60}$	0.21279	−0.08641	5.341	−0.10022	0.06816	35.239
total OF for the propane + n-alkane series			**25.304**			**89.827**
$C_4 + C_{10}$	0.05039	−0.01174	0.756	0.02994	0.01083	0.983
$C_4 + C_{14}$	0.06841	−0.01837	0.008	0.04750	0.01716	0.583
$C_4 + C_{60}$	0.15785	−0.05518	2.300	−0.06928	0.05742	43.317
total OF for the n-butane + n-alkane series			**3.064**			**44.883**

[a]See eqs 13 and 14.

Table 6. Experimental Data Used To Adjust the Volume Shift Parameters

compound	isothermic (K)	isobaric (bar)	volume range (L/mol)	pressure range (bar)	temperature range (K)	N points[a]	reference
C10	283.15−520.15		0.173−0.245	1−2745		66	21−23
C15	311.15−408.15		0.222−0.287	1−6201.9		68	24
C18	352.55−408.15		0.267−0.335	1−5168.2		48	24
C24	353.15−393.15		0.407−0.461	1−1495.5		77	25
C28		1.013−13.80	0.500−0.633		323.15−573.15	10	26,27
C36		1.013	0.642−0.688		373.15−523.15	4	27
C64		1.013	1.185−1.286		423.15−523.15	3	27

[a]Number of experimental data points used to adjust the volume shift parameters.

is dependent on the compositions of each phase or of the overall composition for single-phase mixtures. In this case, the dependence is obtained by calculating a volume translation of the mixture as the average linearly weighted translation according to the molar composition, on the basis of the volume shift of the pure n-alkanes. This is summarized in eq

DOI: 10.1021/acs.jced.8b01050
J. Chem. Eng. Data XXXX, XXX, XXX−XXX

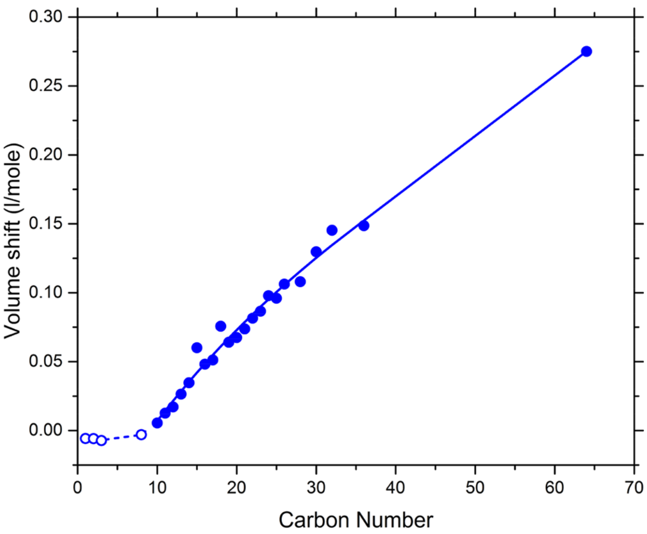

Figure 3. Volume shifts vs carbon number of *n*-alkanes for the RKPR EoS. Filled and empty dots: Average differences between the volumes obtained with the RKPR EoS and the experimental volumes for selected *n*-alkanes. Two regressions were proposed: the first one for *n*-alkanes from C1 to C8 (dashed line) and the second one for *n*-alkanes from *n*-C10 to *n*-C64 (solid line) (see eqs 15 and 16, respectively).

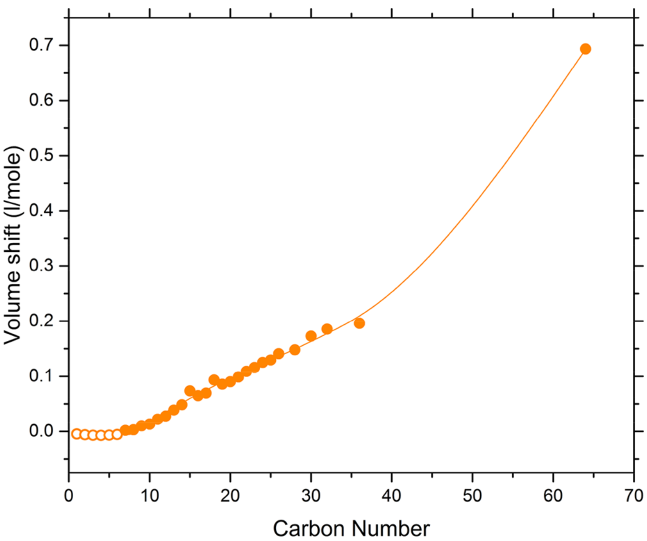

Figure 4. Volume shifts vs carbon number of *n*-alkanes for the PR EoS. Filled dots: Average differences between the volumes obtained with the PR EoS and the experimental volumes obtained for selected *n*-alkanes. Empty dots: For *n*-alkanes from C1 to C6, the volume shifts considered are those proposed by Pedersen et al.[28] For higher *n*-alkanes (*n*-C8 to *n*-C64), a regression is proposed (solid line, see eq 17).

18, where z_{CNi} is the global molar fraction of the *n*-alkane "*i*" for single-phase states, and $V_{shift-CNi}$ is the volume translation of the corresponding pure *n*-alkane.

$$V_{shift-mixture} = \sum z_{CNi} V_{shift-CNi} \tag{18}$$

This equation can be extended to mixtures in biphasic state, but in this case, z_{CNi} would represent the molar fraction of the *n*-alkane in the gas or in the liquid phase, and a mixing volume shift must be calculated for each phase.

■ RESULTS AND DISCUSSION

All critical lines, isothermal Pxy diagrams, and isopleths presented in this section were calculated with either the public

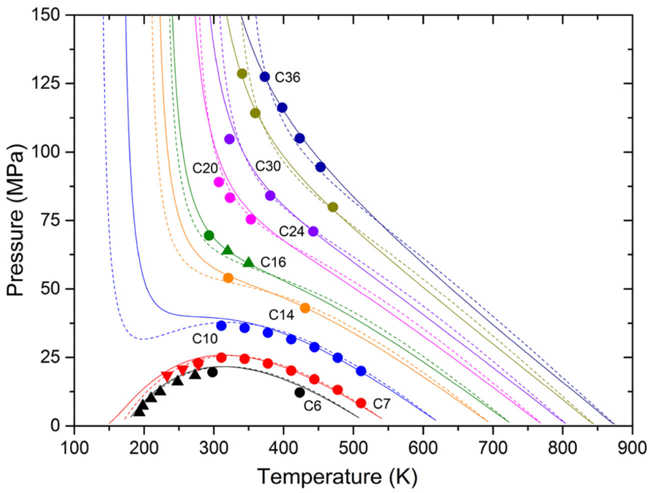

Figure 5. Predicted critical lines for some asymmetric methane + *n*-alkane binary systems. Calculations with the PR (dashed line) and RKPR EoS (solid line) correspond to quadratic mixing rules with parameters from Table 5. Symbols correspond to experimental data from these sources: $C_1 + C_6$;[33,34] $C_1 + C_7$;[35] $C_1 + C_{10}$;[36] $C_1 + C_{14}$;[37] $C_1 + C_{16}$;[38,39] $C_1 + C_{20}$;[8] $C_1 + C_{24}$;[40] $C_1 + C_{30}$;[41] and $C_1 + C_{36}$.[42]

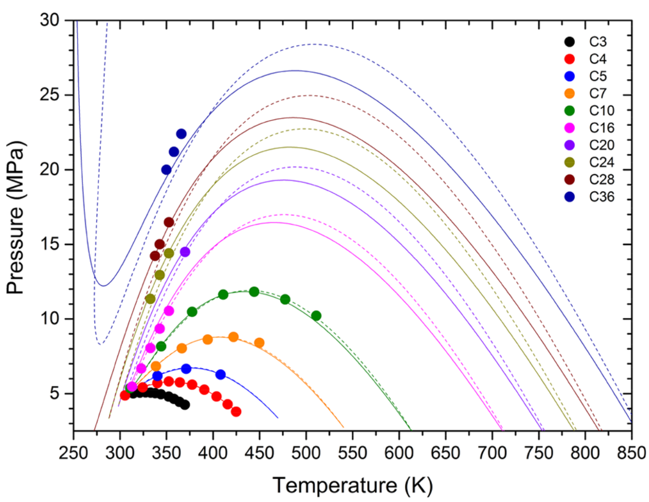

Figure 6. Predicted critical lines for some ethane + *n*-alkane binary systems. Calculations with the PR (dashed line) and RKPR EoS (solid line) correspond to quadratic mixing rules with parameters from Table 5. Symbols correspond to experimental data from these sources: $C_2 + C_3$;[43] $C_2 + C_4$;[43] $C_2 + C_5$;[44] $C_2 + C_7$;[45] $C_2 + C_{10}$;[46] $C_2 + C_{16}$;[47] $C_2 + C_{20}$;[48] $C_2 + C_{24}$;[47] $C_2 + C_{28}$;[47] and $C_2 + C_{36}$.[49]

or in-house versions of GPEC based on algorithms and calculation methods described elsewhere.[30−32]

Binary Series of Methane, Ethane, Propane, and *n*-Butane. Figure 5 presents the calculated critical lines for the more asymmetric systems considered for the methane + *n*-alkane series, both with the PR and RKPR EoS. A very good agreement with experimental data is observed in general for the RKPR EoS. Although these critical lines are quite well-described also with the PR EoS correlations, important differences in the overall performance appear especially in systems from C16 and higher carbon numbers, as can be seen

DOI: 10.1021/acs.jced.8b01050
J. Chem. Eng. Data XXXX, XXX, XXX−XXX

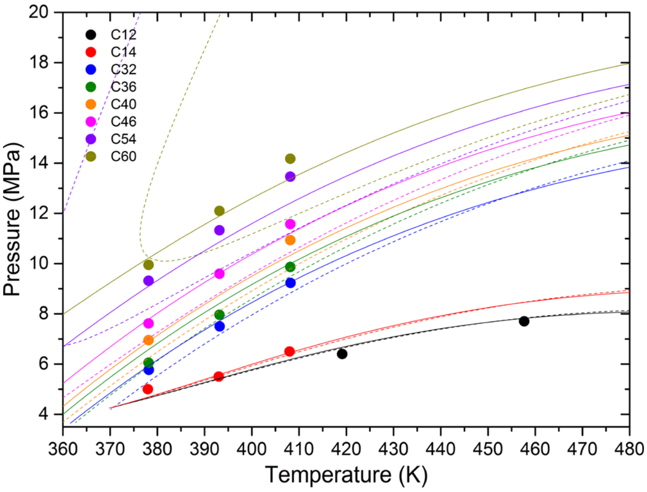

Figure 7. Predicted critical lines for some asymmetric propane + *n*-alkane binary systems. Calculations with the PR EoS (dashed lines) and RKPR EoS (solid line) correspond to quadratic mixing rules with parameters from Table 5. Symbols correspond to experimental data from refs 16 and 50.

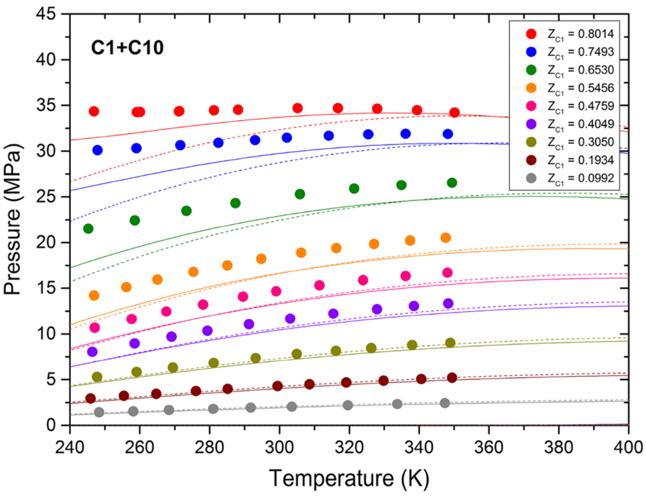

Figure 8. Prediction of isopleths for different C_1 + C_{10} mixtures with the RKPR EoS (solid line) and PR EoS (dashed line) and correlations developed in this work. Symbols: Experimental data from Rijkers et al.[51]

in Table 5, where the value of the contribution to the OF obtained for each of these systems is shown. In the systems with less asymmetry, the performance of both Equations of State is similar. The critical lines calculated with both models for these systems can be consulted in Figure S1 in Section B of the Supporting Information.

Figure 6 shows the critical lines calculated from both models for the ethane + *n*-alkanes homologous series. The predictions from both EoS look quite similar for the lighter systems, but greater deviations are encountered for the heavier systems (from C2 + C20 on), as it can be seen from the individual contributions of these systems to the objective function (see Table 5).

A similar tendency of the EoS predictions is observed for the propane + *n*-alkanes series plotted in Figure 7. Looking at Figure 7, the differences between the PR and PKPR predictions may not be so evident; however, when the individual contributions of the systems to the objective function are analyzed, we observe a higher accuracy of the RKPR EoS to describe the behavior of the heavier systems of this series, particularly from C3 + C20 on.

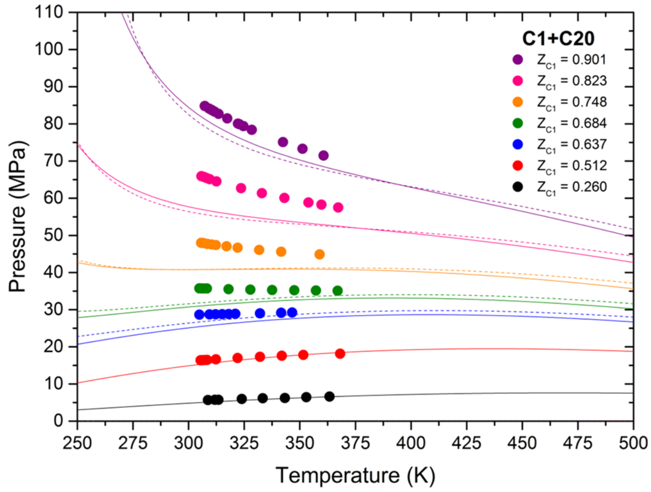

Figure 9. Prediction of isopleths for different C_1 + C_{20} mixtures with the RKPR EoS (solid line) and PR EoS (dashed line) and correlations developed in this work. Symbols: Experimental data from van der Kooi et al.[8]

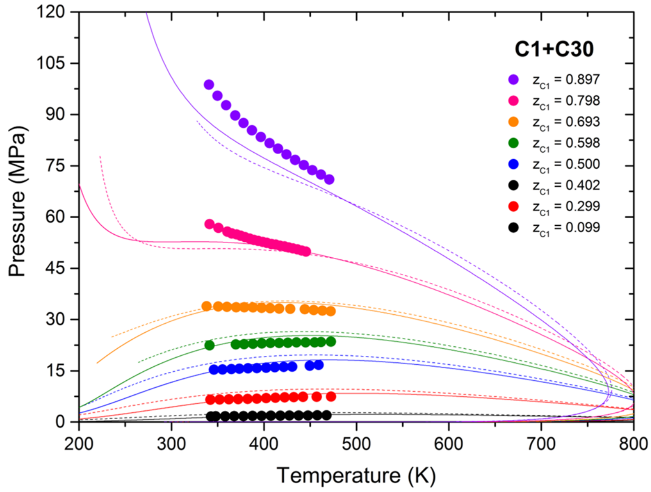

Figure 10. Prediction of isopleths for different C_1 + C_{30} mixtures with the RKPR EoS (solid line) and PR EoS (dashed line) and correlations developed in this work. Symbols: Experimental data from Machado and de Loos.[41]

The RKPR predictions of subcritical vapor−liquid equilibria (VLE) for different methane + *n*-alkane binaries agree very well with experimental data as can be seen in Figures 8−12. In particular, Figures 8−10 show the predictions of isoplethic diagrams of different mixtures of methane + *n*-alkane binary systems. It can be seen that the performance of the RKPR is superior to the performance of PR. These qualitative results are confirmed through the values of the percentage average absolute deviations (AAD) in saturation pressure calculated for these systems (see Table 7). For other methane + *n*-alkane systems, excellent predictions are also shown in Figures S2 to S6 in Section B of the Supporting Information.

Figures 11 and 12 demonstrate a clear superiority of the RKPR correlations for predicting the composition of the light phases or high-pressure solubility of the heavy hydrocarbons in methane, for C_{16} and C_{36}, respectively.

DOI: 10.1021/acs.jced.8b01050
J. Chem. Eng. Data XXXX, XXX, XXX−XXX

Table 7. Comparison of Percentage Average Absolute Deviations (AAD) in Saturation Pressure for Some Asymmetric Systems with the PR and RKPR EoS[a]

system	N_{iso}	T range (K)	P range (bar)	N_{data}[b]	source	% AAD PR2015	RKPR2015	PR2018	RKPR2018
$C_1 + C_{10}$	9	248.33−350.15	14.50−319.05	91	51	3.300	12.811	7.976	8.104
$C_1 + C_{16}$	7	287.74−361.46	41.06−645.60	98	39	4.670	4.415	7.229	10.353
$C_1 + C_{17}$	5	286.25−374.75	100.70−747.10	50	52	7.236	1.837	8.973	9.032
$C_1 + C_{20}$	7	304.88−368.11	163.60−848.20	77	8	17.723	2.375	8.857	7.952
$C_1 + C_{24}$	4	321.24−455.40	103.10−839.00	60	40	21.726	4.043	10.697	5.971
$C_1 + C_{30}$	7	341.27−472.29	16.50−955.00	94	41	33.010	8.124	19.038	6.199
$C_2 + C_{10}$	5	307.90−353.50	32.60−86.60	20	53	3.154	0.704	0.665	2.567
$C_2 + C_{16}$	5	262.25−453.15	5.36−166.10	119	54	13.327	5.430	6.761	3.436
$C_3 + C_{20}$	7	279.29−358.08	4.14−32.47	148	55	12.690	3.053	12.744	3.370
$C_4 + C_{14}$	8	322.77−453.95	1.20−44.03	121	37	5.776	4.942	8.860	4.180
TOTAL	**64**			**787**		**14.126**	**5.832**	**11.147**	**6.635**

[a]With interaction parameters from Tables 3−5 and previous correlations called in this work PR2015 and RKPR2015. [b]The data taken for the calculation are the same as those shown in Figures 8−10, 13, 19, and 21 as well as Figures S2, S3, S4, and S10 (Section B of the Supporting Information) with the exceptions of systems $C_1 + C_{24}$, $C_1 + C_{30}$, $C_2 + C_{10}$, and $C_2 + C_{16}$, for which specific isopleths had to be separated, mainly because RKPR2015 was so off that its performance could not be evaluated for different reasons.

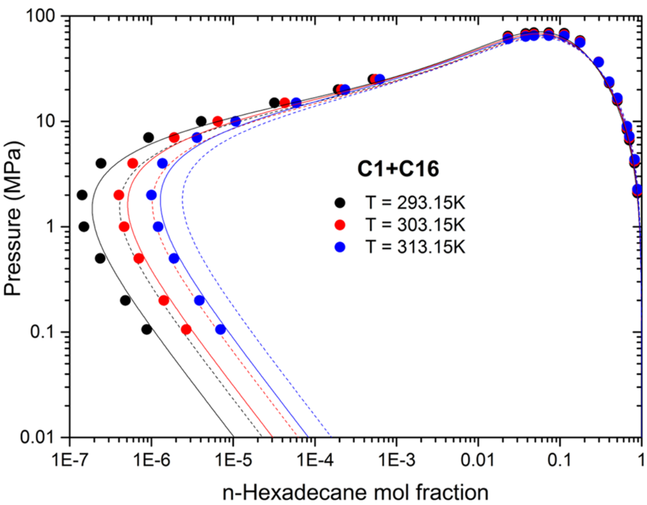

Figure 11. Prediction of isothermal Pxy diagrams for the system $C_1 + C_{16}$ with the RKPR EoS (solid line) and PR EoS (dashed line) and correlations developed in this work. Symbols: Experimental data from Rijkers et al.[38]

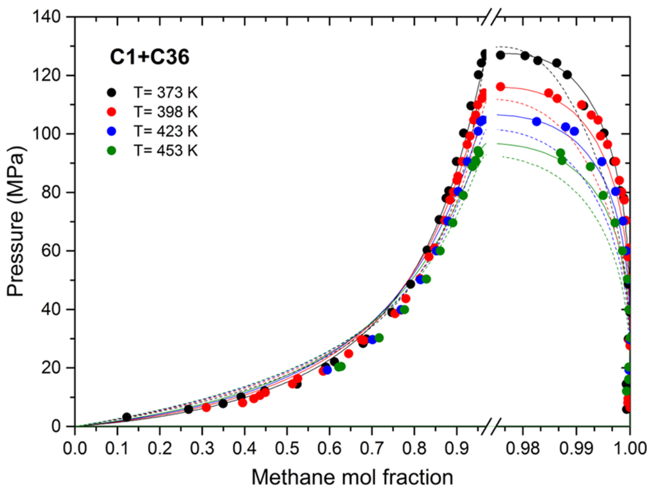

Figure 12. Prediction of isothermal Pxy diagrams for the system $C_1 + C_{36}$ with the RKPR EoS (solid line) and PR EoS (dashed line) and correlations developed in this work. Symbols: Experimental data from Marteau et al.[42]

Figures 13−17 and also Figures S7−S12 in Section B of the Supporting Information show different isoplethic and isothermal Pxy diagrams over a wide range of carbon numbers for the ethane + n-alkane series. In general, the performance of the RKPR is better than that of PR EoS, except in the $C_2 + C_{10}$ system, where the value of the deviations in saturation pressure (AAD) is slightly higher for the RKPR model (see Table 7). However, the value of the total OF for the entire optimized ethane + n-alkanes series is substantially lower for the RKPR EoS, as can be seen in Table 5.

In particular, for the more asymmetric systems, Figures 14−17 as well as Figures S11 and S12 in the Section B of the Supporting Information expose a systematic overprediction of bubble pressures in the whole composition range with the PR EoS, while the new RKPR correlations provide higher accuracy in their predictions. And again, as already observed for the methane series, Figure 17 clearly shows a better description of the light phase composition and also of the critical region with RKPR, in this case, for $C_2 + C_{36}$.

Figures 18−20 show predictions of some binary systems belonging to the series of propane + n-alkanes. As in the previous cases, the better overall performance of the RKPR over the PR remains. As in the previous series Figure 19 illustrates for $C_3 + C_{20}$ a systematic overprediction of bubble pressures by the PR correlations, contrasting with accurate predictions of the RKPR EoS. In the Pxy diagram corresponding to the critical region of system $C_3 + C_{54}$ (Figure 20), it is observed that greater deviations occur at higher temperatures for both models. Nevertheless, it is clear how the experimental behavior is better captured by the RKPR correlations for the three isotherms.

Figures S13 to S21 in Section B of the Supporting Information show additional predictions of the propane + n-alkane series.

The experimental data available for the butane + n-alkane series is less abundant compared to that available for the first three series; however, the predictions with RKPR in this series were equally good and even better in the case of the $C_4 + C_{60}$ system. The trends already observed for the previous series

DOI: 10.1021/acs.jced.8b01050
J. Chem. Eng. Data XXXX, XXX, XXX−XXX

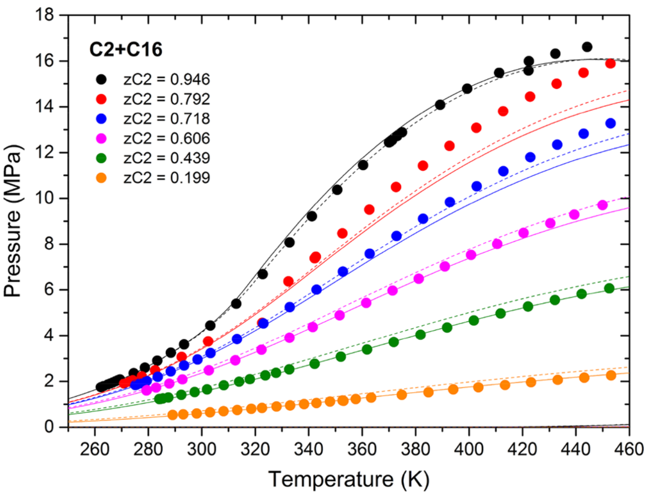

Figure 13. Prediction of isopleths for different C_2 + C_{16} mixtures with the RKPR EoS (solid line) and PR EoS (dashed line) and correlations developed in this work. Symbols Experimental data from Goede et al.[54]

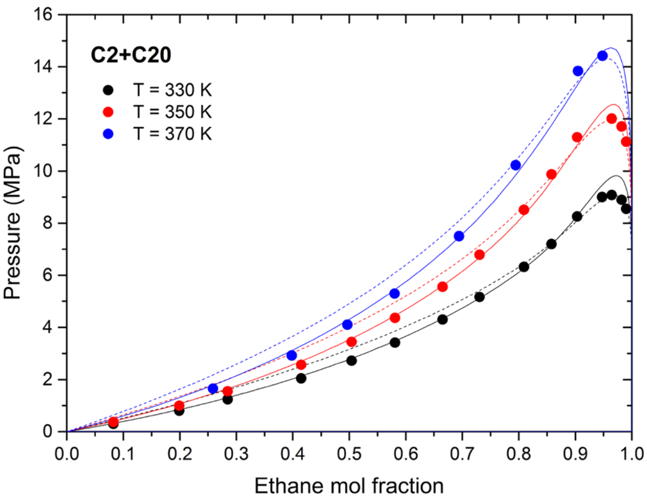

Figure 14. Prediction of isothermal Pxy diagrams for the system C_2 + C_{20} with the RKPR EoS (solid line) and PR EoS (dashed line) and correlations developed in this work. Symbols: Experimental data from Peters et al.[48]

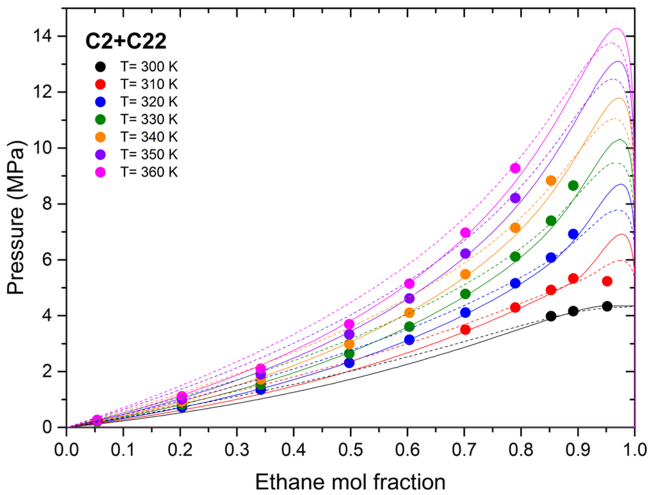

Figure 15. Prediction of isothermal Pxy diagrams for the system C_2 + C_{22} with the RKPR EoS (solid line) and PR EoS (dashed line) and correlations developed in this work. Symbols: Experimental data from Peters et al.[56]

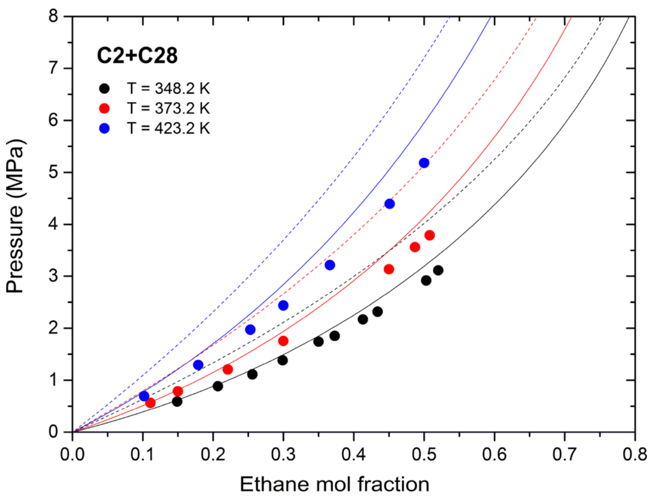

Figure 16. Prediction of isothermal Pxy diagrams for the system C_2 + C_{28} with the RKPR EoS (solid line) and PR EoS (dashed line) and correlations developed in this work. Symbols: Experimental data from Gasem et al.[57]

regarding bubble pressures are once again confirmed in both figures, involving C_4 + C_{14} (Figure 21) and C_4 + C_{60} (Figure 22).

Binary Series of Higher *n*-Alkanes. For simplification, as already explained in the previous section, from the series of *n*-hexane + *n*-alkanes, the interaction parameters k'_{ij} and k_{ij}^{inf} were considered null. The high-pressure VLE behavior in mixtures of *n*-hexane also seems to be properly captured by the proposed correlations, as it can be seen from the prediction of the critical lines in Figure 23 and the isothermal Pxy diagrams for the more asymmetric systems compared to the available data (Figures 24 and 25).

Volume Translations Results. For a more accurate prediction of volumetric properties, a volume translation strategy was implemented for both EoS used in this work, i.e., PR EoS and RKPR EoS, according to the procedure described in the Methodology and Parametrization Strategy section.

Figure 26 shows the volume−composition curve for a mixture of methane + *n*-decane at 373.15 K and 1000 bar. The volumes were obtained with the PR (dashed lines) and RKPR (solid line) models (parameters in Table 5) and volume translations were applied (see eqs 15−18). The dots in Figure 26, the same as for Figure 1, correspond to the experimental data of ref 7. From Figure 26, we observe that the predicted volumes, through both models, follow the almost linear behavior seen in the experimental data. Moreover, in the upper part of Figure 26, we observe that small negative excess volumes are predicted by both PR and RKPR, which is in accordance with the trend exposed by the data when a second-order regression is applied. Then, the elimination of the *lij* interaction parameter in the new correlation of RKPR EoS presented in this work seems to have solved the previously mentioned drawback detected for the RKPR2015 correlations. Now, we observe an accurate prediction of fluid phase equilibria, as previously shown, and also of mixture liquid volumes with the same model.

DOI: 10.1021/acs.jced.8b01050
J. Chem. Eng. Data XXXX, XXX, XXX−XXX

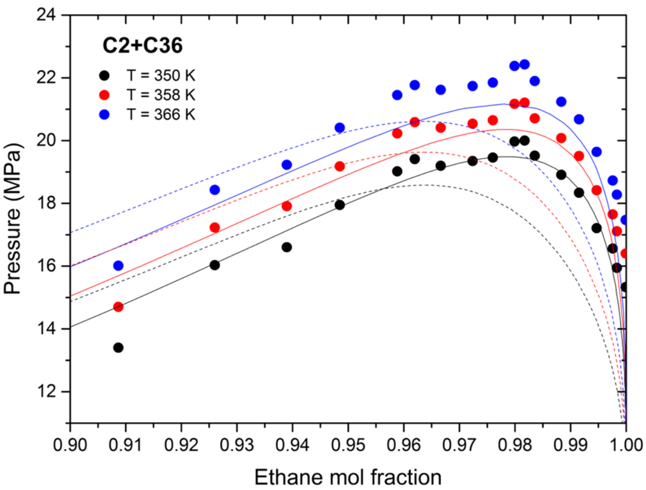

Figure 17. Prediction of isothermal Pxy diagrams for the system C_2 + C_{36} with the RKPR EoS (solid line) and PR EoS (dashed line) and correlations developed in this work. Symbols: Experimental data from Schwarz et al.[49]

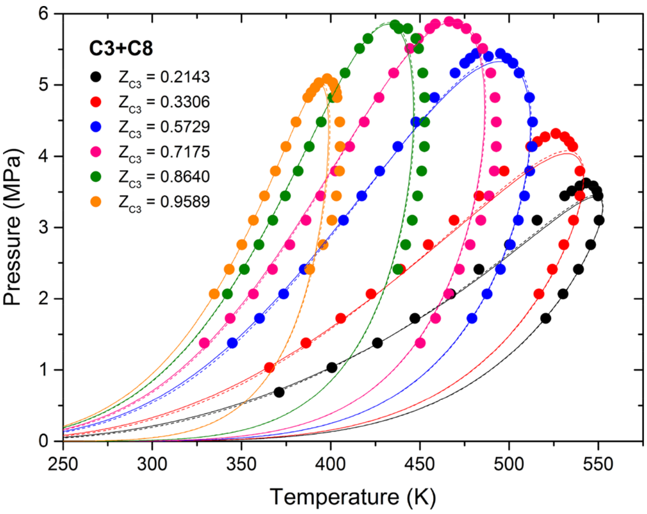

Figure 18. Prediction of isopleths for different C_3 + C_8 mixtures with the RKPR EoS (solid line) and PR EoS (dashed line) and correlations developed in this work. Symbols: Experimental data from Kay et al.[58]

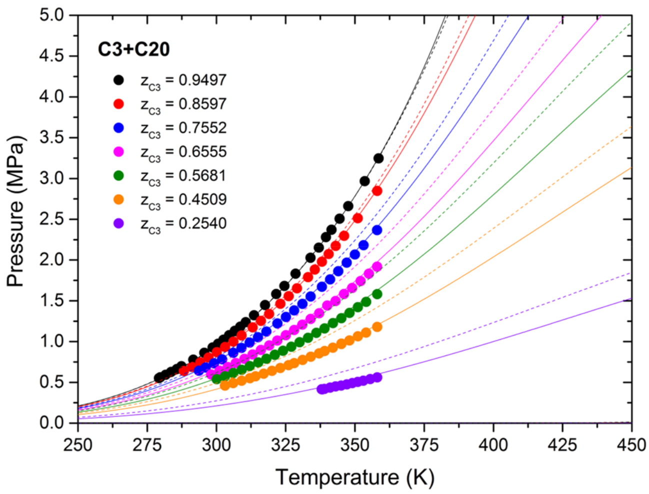

Figure 19. Prediction of isopleths for different C_3 + C_{20} mixtures with the RKPR EoS (solid line) and PR EoS (dashed line) and correlations developed in this work. Symbols: Experimental data from Gregorowicz et al.[55]

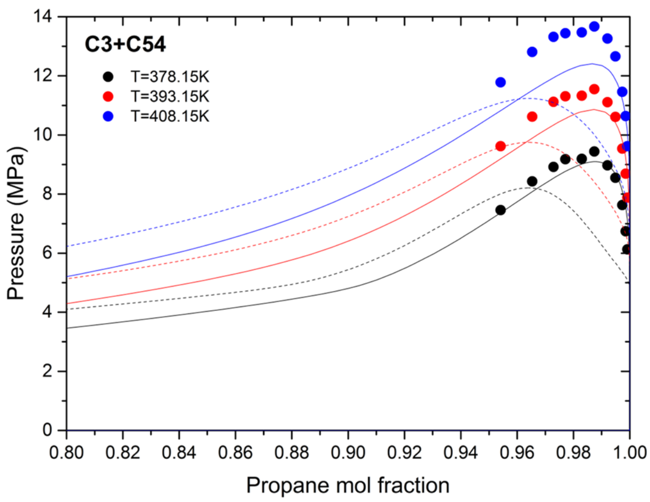

Figure 20. Prediction of isothermal Pxy diagrams for the system C_3 + C_{54} with the RKPR EoS (solid line) and PR EoS (dashed line) and correlations developed in this work. Symbols: Experimental data from Schwarz and Nieuwoudt.[16]

Figure 27 shows the predicted translated volumes for a mixture of methane + *n*-decane at 373.15 K at four different compositions. The volumes predicted by the PR EoS (dashed lines) and RKPR EoS (solid line) are quite similar in this case. A slightly better match with the experimental data is observed for the PR model at the higher pressure range and for the RKPR model at lower pressures.

Figure 28 shows the predicted translated volumes for a mixture of ethane + *n*-decane with an ethane mole fraction of z_1 = 0.9 at four different temperatures. In this case, the volumes predicted by RKPR EoS (solid line) are closer to the experimental data of ref 46 than the volumes predicted by the PR EoS (dashed lines). The RKPR predictions are superior in the whole pressure range of Figure 28.

Additional volumetric predictions based on the same volume shift correlations are presented in Section C of the Supporting Information, considering both pure compounds and binary mixtures. It can be seen that both models with the new correlated parameters allow for a proper description of mixture liquid volumes once volume shifts are applied. Although the conditions of Figures 26–28 were selected for illustrative purposes, the implementation of a temperature-dependent volume translation would allow for an accurate prediction of mixture volumes in wide ranges of temperatures.

Correction of Solid–Fluid Equilibrium Predictions. The same mixture and data considered in Figure 1 are now revisited in Figure 29, including predictions with RKPR2018. In the calculations performed for preparing both figures, literature data for the melting temperature, enthalpy, and volume changes of fusion of *n*-eicosane were used for the calculation of its pure solid fugacity. From Figure 29, it can be clearly seen how the slope of this isopleth has been corrected on the basis of the new correlation without *lij* interactions proposed in this work. Consider also that these are just predictions with a simple and straightforward treatment of the solid fugacity. A systematic work focused on the modeling of solid–fluid behaviors for this type of mixtures is on preparation.

DOI: 10.1021/acs.jced.8b01050
J. Chem. Eng. Data XXXX, XXX, XXX–XXX

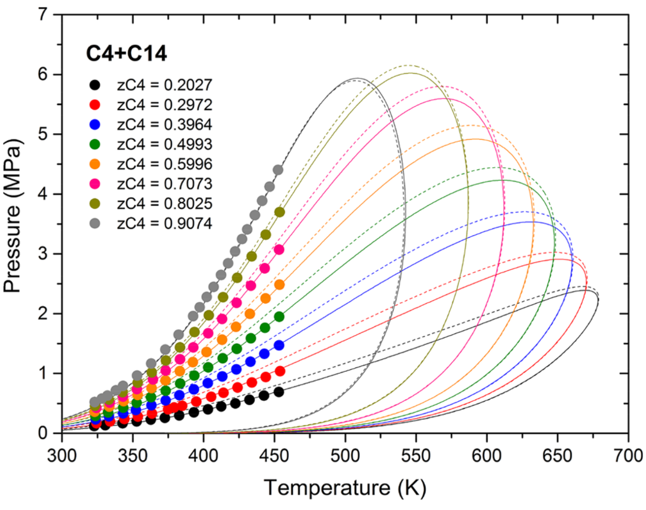

Figure 21. Prediction of isopleths for different C_4 + C_{14} mixtures with the RKPR EoS (solid line) and PR EoS (dashed line) and correlations developed in this work. Symbols: Experimental data from de Leeuw et al.[37]

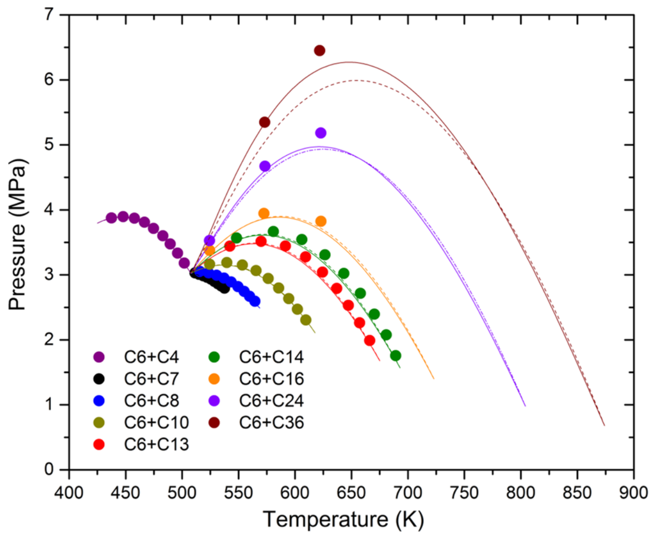

Figure 23. Critical lines for some n-hexane + n-alkane binary systems. Calculations with the PR EoS (dashed lines) and RKPR EoS (solid line) correspond to quadratic mixing rules with null interaction parameters. Symbols: Experimental data from refs 60−62.

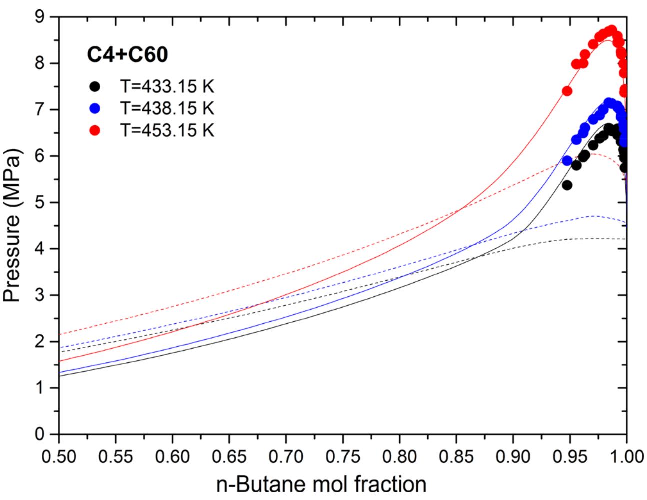

Figure 22. Prediction of isothermal Pxy diagrams for the system C_4 + C_{60} with the RKPR EoS (solid line) and PR EoS (dashed line) and correlations developed in this work. Symbols: Experimental data from Nieuwoudt.[59]

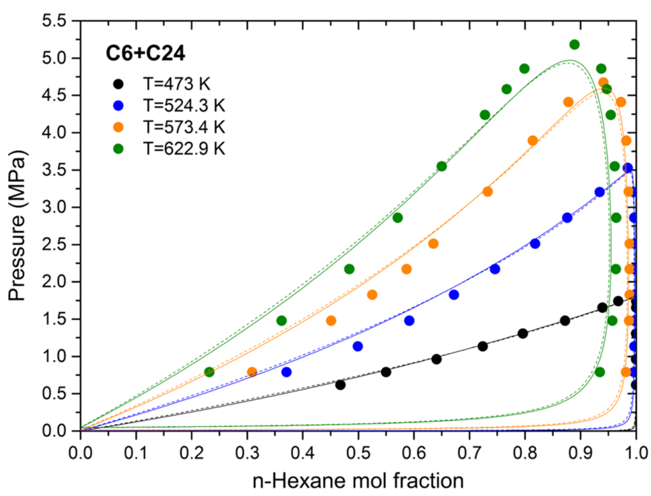

Figure 24. Prediction of isothermal Pxy diagrams for the system C_6 + C_{24} with the RKPR EoS (solid line) and PR EoS (dashed line) with null interaction parameters. Symbols: Experimental data from ref 61.

■ CONCLUSIONS

In this work, new parametrizations of the RKPR and the PR EoS were developed and presented for n-alkane mixtures. This includes the development of new correlations of temperature-dependent *kij* attractive parameters for all possible pairs of normal alkanes together with null *lij* repulsive parameters or, in other words, a linear mixing rule for the covolume. For the case of the RKPR EoS, a new correlation for the structural δ_1 parameter as a function of the n-alkane carbon number was also proposed, to be used together with tabulated values of critical temperature and pressure, plus acentric factor, in the estimation of pure compound parameters.

The correlations obtained for the PR EoS yield much larger values for the optimized objective function in comparison to those obtained for the RKPR EoS for the homologue series of methane, ethane, propane, and n-butane + n-alkanes. Predictions for the first group of systems along each series are in general good and quite similar between both models. Nevertheless, a quite systematic tendency to overestimate bubble pressures of the more asymmetric systems of each series was observed in this work for the PR model, starting at approximately C20, C16, and C14 for the series of methane, ethane, and propane, respectively. In turn, having followed exactly the same methodology in developing the correlations for both models, using a mix of critical and far from critical experimental data in the objective functions, RKPR achieves a more appropriate description of both types of regions. Besides providing more accurate predictions for bubble pressures, the new RKPR correlations describe at the same time the critical region and light phases in general much better than PR does.

These different results can be ascribed to the third parameter in the RKPR model and how it evolves along the alkane family of compounds, to represent from simple small near-spherical molecules up to very long chains. Although the δ_1 parameter does not have a clear theoretical meaning as the m parameter in SAFT type models, its role is completely analogous, and in

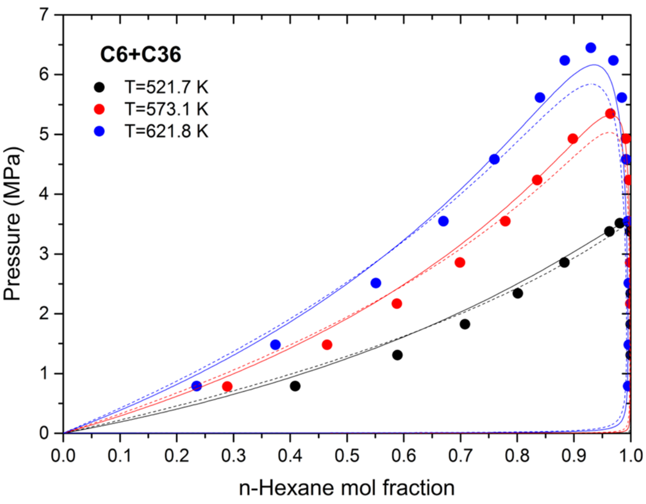

Figure 25. Prediction of isothermal Pxy diagrams for the system C_6 + C_{36} with the RKPR EoS (solid line) and PR EoS (dashed line) with null interaction parameters. Symbols: Experimental data from ref 61.

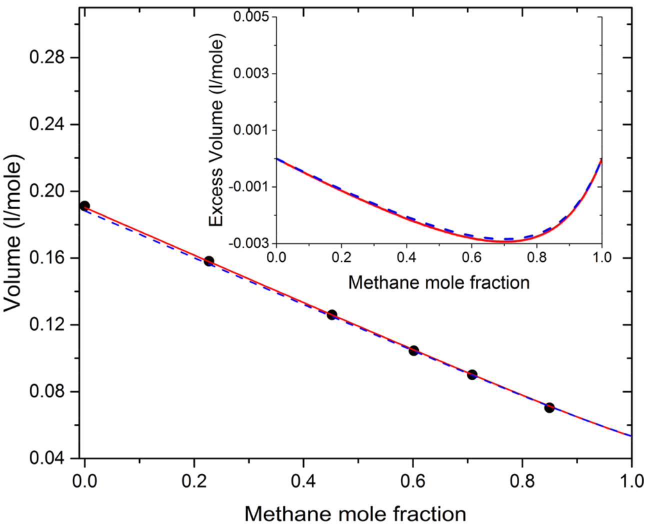

Figure 26. Mixture molar volume and excess volume for the system methane + *n*-decane at 373.15 K and 1000 bar. Calculations with the PR EoS (dashed lines) and RKPR EoS (solid line) correspond to quadratic mixing rules with parameters from Table 5 and volume translations according to eq 18. Dots: Experimental data from ref 7.

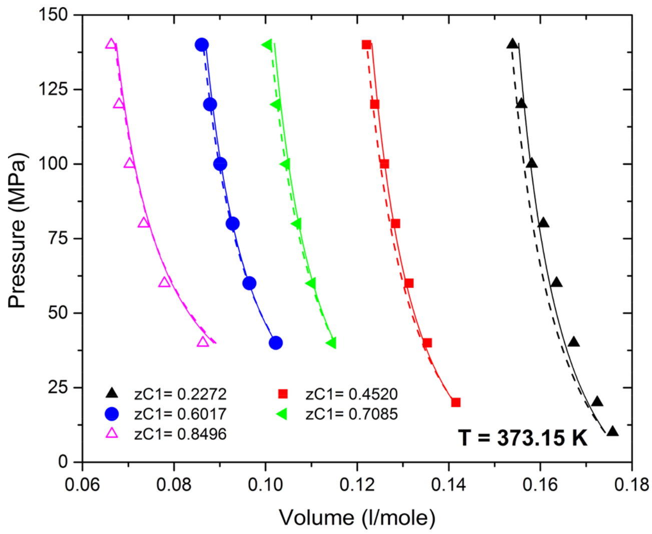

Figure 27. Pressure vs translated volume projection for the system methane (1) + *n*-decane (2) at 373.15 K. The predicted volumes correspond to the PR EoS (dashed lines) and RKPR EoS (solid line) models considering the parameters of Table 5 and the volume translations performed according to eq 18. Symbols: Experimental data from ref 7.

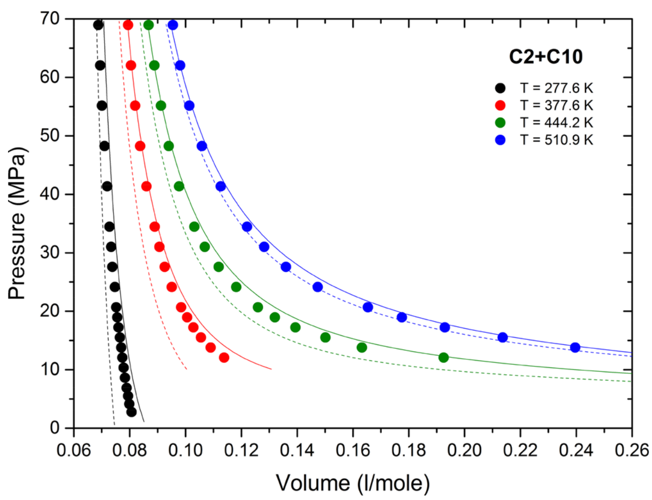

Figure 28. Pressure vs translated volume projection for the system ethane (1) + *n*-decane (2) with an ethane mole fraction z_1 = 0.9. The predicted volumes correspond to the PR EoS (dashed lines) and RKPR EoS (solid line) models considering the parameters of Table 5 and the volume translations performed according to eq 18. Symbols: Experimental data from ref 46.

this work, it was used in an engineering practical way. In other words, equations like SRK or PR are in essence corresponding states models,[5] as would also be the case for a "SAFT" type model where *m* is a universal constant instead of a pure compound parameter, and therefore, they should not be used for modeling asymmetric mixtures.

Moreover, and different to the RKPR2015 correlations,[1] the present results could be achieved without recurring to a nonlinear mixing rule for the covolume, and as already discussed, this also provides a good and consistent base for modeling volumetric properties as well as solid−fluid equilibria.

In summary, besides minor changes and extensions in the data sets considered, the main difference with respect to the RKPR2015 correlations lies in not using *lij* parameters while the *kij* function is now allowed to converge to nonzero values at infinite temperature. In other words, parametrically speaking, we replaced the *lij* interaction with the k_{ij}^{inf}. And together with that, there is a new correlation for the δ_1 parameter, which increases monotonically with carbon number instead of presenting a maximum. The new correlations allow a model capable of describing the phase as well as the volumetric behaviors of hydrocarbon mixtures, even for the more asymmetric systems, which are not properly represented by the classic EoS (SKR or PR). For simplification, null interactions are applied to the higher *n*-alkanes series from C6 on, with very good results confirmed in particular for the *n*-hexane series.

Thus, the correlations presented in this work provide a good and consistent base for developing more complete models that can predict phase behavior and volumetric properties of

DOI: 10.1021/acs.jced.8b01050
J. Chem. Eng. Data XXXX, XXX, XXX−XXX

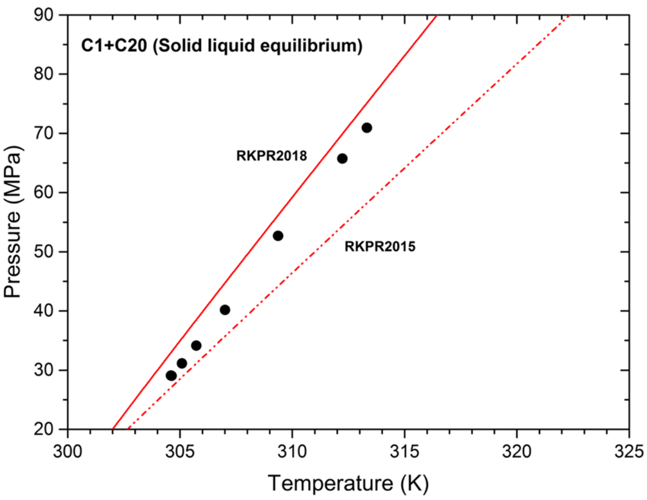

Figure 29. Predicted solid−liquid phase envelope for a mixture of methane + *n*-eicosane, with mole fractions of 0.637 and 0.363, respectively. Calculations with the RKPR2015 (dotted-dashed lines) and RKPR2018 (solid line). Dots: Experimental data from ref 8.

hydrocarbon mixtures of known composition and correlate the same type of properties for real reservoir fluids.

The use of the previous correlations here denoted RKPR2015 can be recommended only for the more asymmetric binary systems of the methane series, i.e., with carbon numbers around 16 or higher, if the volumetric properties and solid−fluid equilibria are not of interest. Otherwise, the new correlations proposed in the present work represent the best compromise for the description of all studied mixtures and properties.

ASSOCIATED CONTENT

Supporting Information

The Supporting Information is available free of charge on the ACS Publications website at DOI: 10.1021/acs.jced.8b01050.

Section A: Tables containing selected data for objective functions; Section B: Complementary figures; Section C: Additional volume shift results (PDF)

AUTHOR INFORMATION

Corresponding Author

*E-mail: martin.cismondi@unc.edu.ar; martin.cismondi.d@ypftecnologia.com.

ORCID

Martín Cismondi: 0000-0002-9349-8594

Funding

M.C. and N.G.T. acknowledge the financial support received from Consejo Nacional de Investigaciones Científicas y Técnicas de la República Argentina (CONICET) Grant PIP (2015) 112-201501-00923CO, Agencia Nacional de Promoción Científica y Tecnológica (ANPCyT) Grant PICT-2016-1521, and Universidad Nacional de Córdoba (UNC). S.B.R.B. acknowledges the funding received from CONICET Grant PIP (2016) 11220150100918CO, ANPCyT Grant PICT-2017-1235, and Universidad Nacional del Sur (UNS) Grant PGI-24/M148.

Notes

The authors declare no competing financial interest.

REFERENCES

(1) Cismondi Duarte, M.; Cruz Doblas, J.; Gomez, M. J.; Montoya, G. F. Modelling the Phase Behavior of Alkane Mixtures in Wide Ranges of Conditions: New Parameterization and Predictive Correlations of Binary Interactions for the RKPR EOS. *Fluid Phase Equilib.* **2015**, *403*, 49−59.

(2) Soave, G. Equilibrium Constants from a Modified Redlich-Kwong Equation of State. *Chem. Eng. Sci.* **1972**, *27* (6), 1197−1203.

(3) Peng, D. Y.; Robinson, D. B. A New Two-Constant Equation of State. *Ind. Eng. Chem. Fundam.* **1976**, *15* (1), 59−64.

(4) Cismondi Duarte, M.; Galdo, M. V.; Gomez, M. J.; Tassin, N. G.; Yanes, M. High Pressure Phase Behavior Modeling of Asymmetric Alkane+alkane Binary Systems with the RKPR EOS. *Fluid Phase Equilib.* **2014**, *362*, 125−135.

(5) Cismondi, M.; Mollerup, J. Development and Application of a Three-Parameter RK-PR Equation of State. *Fluid Phase Equilib.* **2005**, *232* (1−2), 74−89.

(6) Tassin, N. G.; Mascietti, V. A.; Cismondi, M. Phase Behavior of Multicomponent Alkane Mixtures and Evaluation of Predictive Capacity for the PR and RKPR EoS ' S. *Fluid Phase Equilib.* **2019**, *480*, 53−65.

(7) Regueira, T.; Pantelide, G.; Yan, W.; Stenby, E. H. Density and Phase Equilibrium of the Binary System Methane + N-Decane under High Temperatures and Pressures. *Fluid Phase Equilib.* **2016**, *428*, 48−61.

(8) van der Kooi, H. J.; Flöter, E.; de Loos, Th. W. High-Pressure Phase Equilibria of (1-x)CH4 + XCH3(CH2)18CH3. *J. Chem. Thermodyn.* **1995**, *27* (4), 847−861.

(9) Michelsen, M. L.; Mollerup, J. M. *Thermodynamic Models: Fundamentals & Computacional Aspects*, 2nd ed.; 2007.

(10) Yang, F.; Liu, Q.; Duan, Y.; Yang, Z. On the Temperature Dependence of the Alpha Function in the Cubic Equation of State. *Chem. Eng. Sci.* **2018**, *192*, 565−575.

(11) Martinez, S. A.; Hall, K. R. Thermodynamic Properties of Light Synthetic Natural Gas Mixtures Using the RK-PR Cubic Equation of State. *Ind. Eng. Chem. Res.* **2006**, *45*, 3684−3692.

(12) Arendsen, A. R. J.; Versteeg, G. F. Dynamic Thermodynamics with Internal Energy, Volume, and Amount of Moles as States: Application to Liquefied Gas Tank. *Ind. Eng. Chem. Res.* **2009**, *48* (6), 3167−3176.

(13) Kim, S. K.; Choi, H. S.; Kim, Y. Thermodynamic Modeling Based on a Generalized Cubic Equation of State for Kerosene/LOx Rocket Combustion. *Combust. Flame* **2012**, *159* (3), 1351−1365.

(14) Cismondi, M.; Mollerup, J. M.; Zabaloy, M. S. Equation of State Modeling of the Phase Equilibria of Asymmetric CO2 + N-Alkane Binary Systems Using Mixing Rules Cubic with Respect to Mole Fraction. *J. Supercrit. Fluids* **2010**, *55* (2), 671−681.

(15) Cismondi, M.; Rodriguez Reartes, S. B.; Milanesio, J. M.; Zabaloy, M. S. Phase Equilibria of CO2 + n -Alkane Binary Systems in Wide Ranges of Conditions: Development of Predictive Correlations Based on Cubic Mixing Rules. *Ind. Eng. Chem. Res.* **2012**, *51*, 6232−6250.

(16) Schwarz, C. E.; Nieuwoudt, I. Phase Equilibrium of Propane and Alkanes Part II: Hexatriacontane through Hexacontane. *J. Supercrit. Fluids* **2003**, *27*, 145−156.

(17) Péneloux, A.; Rauzy, E.; Fréze, R. A Consistent Correction for Redlich-Kwong-Soave Volumes. *Fluid Phase Equilib.* **1982**, *8* (1), 7−23.

(18) Zabaloy, M. S.; Brignole, E. A. On Volume Translations in Equations of State. *Fluid Phase Equilib.* **1997**, *140* (1−2), 87−95.

(19) Jaubert, J. N.; Privat, R.; Le Guennec, Y.; Coniglio, L. Note on the Properties Altered by Application of a Péneloux-Type Volume Translation to an Equation of State. *Fluid Phase Equilib.* **2016**, *419*, 88−95.

(20) Span, R.; Wagner, W. Equations of State for Technical Applications. II. Results for Nonpolar Fluids. *Int. J. Thermophys.* **2003**, *24* (1), 41−109.

DOI: 10.1021/acs.jced.8b01050
J. Chem. Eng. Data XXXX, XXX, XXX−XXX

(21) Troncoso, J.; Bessieres, D.; Cerdeiriña, C. A.; Carballo, E.; Romanı, L. PpTx Data for the Dimethyl Carbonate + Decane System. *J. Chem. Eng. Data* **2004**, *49*, 923−927.

(22) Segovia, J. J.; Fandiño, O.; López, E. R.; Lugo, L.; Carmen Martin, M.; Fernández, J. Automated Densimetric System: Measurements and Uncertainties for Compressed Fluids. *J. Chem. Thermodyn.* **2009**, *41* (5), 632−638.

(23) Liu, K.; Wu, Y.; McHugh, M. A.; Baled, H.; Enick, R. M.; Morreale, B. D. Equation of State Modeling of High-Pressure, High-Temperature Hydrocarbon Density Data. *J. Supercrit. Fluids* **2010**, *55*, 701−711.

(24) Cutler, W. G.; McMickle, R. H.; Webb, W.; Schiessler, R. W. Study of the Compressions of Several High Molecular Weight Hydrocarbons. *J. Chem. Phys.* **1958**, *29* (4), 727−740.

(25) Dutour, S.; Lagourette, B.; Daridon, J. L. High-Pressure Speed of Sound and Compressibilities in Heavy Normal Hydrocarbons: N-C23H48 and n-C24H50. *J. Chem. Thermodyn.* **2001**, *33*, 765−774.

(26) Rodden, J. B.; Erkey, C.; Akgerman, A. Mutual Diffusion Coefficients for Several Dilute Solutes in N-Octacosane and the Solvent Density at 371−534 K. *J. Chem. Eng. Data* **1988**, *33* (4), 450−453.

(27) Doolittle, K.; Peterson, R. H. Preparation and Physical Properties of a Series of N-Alkanes. *J. Am. Chem. Soc.* **1951**, *73* (5), 2145−2151.

(28) Pedersen, K. S.; Christensen, P. L.; Shaikh, J. A. *Phase Behaviour of Petroleum Reservoir Fluids*, 2nd ed.; Taylor & Francis Group, LLC., 2014.

(29) AIChE. *DIPPR 801 Database*. Evaluated Process Design Data, Public Release in, American Institute of Chemical Engineers, Design Institute for Physical Property Data, BYU-DIPPR, Thermophysical Properties Laboratory: Provo, UT, 2003.

(30) Cismondi, M.; Michelsen, M. L. Global Phase Equilibrium Calculations: Critical Lines, Critical End Points and Liquid−liquid−vapour Equilibrium in Binary Mixtures. *J. Supercrit. Fluids* **2007**, *39* (3), 287−295.

(31) Cismondi, M.; Michelsen, M. Automated Calculation of Complete Pxy and Txy Diagrams for Binary Systems. *Fluid Phase Equilib.* **2007**, *259* (2), 228−234.

(32) Cismondi, M.; Michelsen, M. L.; Zabaloy, M. S. Automated Generation of Phase Diagrams for Binary Systems with Azeotropic Behavior. *Ind. Eng. Chem. Res.* **2008**, *47* (23), 9728−9743.

(33) Shim, J.; Kohn, J. P. Multiphase and Volumetric Equilibria of Methane-n-Hexane Binary System at Temperatures between −110 and 150 °C. *J. Chem. Eng. Data* **1962**, *7* (1), 3−8.

(34) Chen, R. J. J.; Chappelear, P. S.; Kobayashi, R. Dew-Point Loci for Methane-n-Hexane and Methane-n-Heptane Binary Systems. *J. Chem. Eng. Data* **1976**, *21* (2), 213−219.

(35) Reamer, H. H.; Sage, B. H.; Lacey, W. N. Volumetric and Phase Behavior of the Methane-n-Heptane System. *Chem. Eng. Data Ser.* **1956**, *1* (1), 29−42.

(36) Reamer, H. H.; Olds, R. H.; Sage, B. H.; Lacey, W. N. Phase Equilibria in Hydrocarbon Systems. Methane-Decane System. *Ind. Eng. Chem.* **1942**, *34* (12), 1526−1531.

(37) de Leeuw, V. V.; de Loos, T. W.; Kooijman, H. A.; de Swaan Arons, J. The Experimental Determination and Modelling of VLE for Binary Subsystems of the Quaterhary System N2 + CH4 + C4H10 + C14H30 UP to 1000 bar and 440 K. *Fluid Phase Equilib.* **1992**, *73* (3), 285−321.

(38) Rijkers, M. P. W. M.; Peters, C. J.; de Swaan Arons, J. Measurements on the Phase Behavior of Binary Mixtures for Modeling the Condensation Behavior of Natural Gas. Part III. The System Methane + Hexadecane. *Fluid Phase Equilib.* **1993**, *85* (C), 335−345.

(39) Glaser, M.; Peters, C. J.; Van Der Kool, H. J.; Lichtenthaler, R. N. Phase Equilibria of (Methane + n-Hexadecane) and (p, Vm, T) of n-Hexadecane. *J. Chem. Thermodyn.* **1985**, *17* (9), 803−815.

(40) Flöter, E.; De Loos, T. W.; De Swaan Arons, J. High Pressure Solid-Fluid and Vapour-Liquid Equilibria in the System (Methane + Tetracosane). *Fluid Phase Equilib.* **1997**, *127* (1−2), 129−146.

(41) Machado, J. J. B.; De Loos, T. W. Liquid-Vapour and Solid-Fluid Equilibria for the System Methane + Triacontane at High Temperature and High Pressure. *Fluid Phase Equilib.* **2004**, *222−223*, 261−267.

(42) Marteau, P.; Tobaly, P.; Ruffier-Meray, V.; De Hemptinne, J. C. High-Pressure Phase Diagrams of Methane + Squalane and Methane + Hexatriacontane Mixtures. *J. Chem. Eng. Data* **1998**, *43* (3), 362−366.

(43) Horstmann, S.; Fischer, K.; Gmehling, J. Experimental Determination of Critical Data of Mixtures and Their Relevance for the Development of Thermodynamic Models. *Chem. Eng. Sci.* **2001**, *56* (24), 6905−6913.

(44) Ekiner, O.; Thodos, G. Critical Temperatures and Critical Pressures of the Ethane-n-Pentane System. *J. Chem. Eng. Data* **1966**, *11* (2), 154−155.

(45) Mehra, V. S.; Thodos, G. Vapor-Liquid Equilibrium in Ethane n-Butane System. *J. Chem. Eng. Data* **1965**, *10* (4), 307−309.

(46) Reamer, H. H.; Sage, B. H. Phase Equilibria in Hydrocarbon Systems: Volumetric and Phase Behavior of the Ethane-n-Decane System. *J. Chem. Eng. Data* **1962**, *7* (2), 161−168.

(47) Nieuwoudt, I.; Du Rand, M. Measurement of Phase Equilibria of Supercritical Carbon Dioxide and Paraffins. *J. Supercrit. Fluids* **2002**, *22* (3), 185−199.

(48) Peters, C. J.; De Roo, J. L.; Lichtenthaler, R. N. Measurements and Calculations of Phase Equilibria of Binary Mixtures of Ethane + Eicosane. Part I: Vapour + Liquid Equilibria. *Fluid Phase Equilib.* **1987**, *34* (2−3), 287−308.

(49) Schwarz, C. E.; Nieuwoudt, I.; Knoetze, J. H. Phase Equilibria of Long Chain N-Alkanes in Supercritical Ethane: Review, Measurements and Prediction. *J. Supercrit. Fluids* **2008**, *46* (3), 226−232.

(50) Schwarz, C. E.; Nieuwoudt, I. Phase Equilibrium of Propane and Alkanes. Part I. Experimental Procedures, Dotriacontane Equilibrium and EOS Modelling. *J. Supercrit. Fluids* **2003**, *27*, 133−144.

(51) Rijkers, M. P. W. M.; Malais, M.; Peters, C. J.; de Swaan Arons, J. Measurements on the Phase Behavior of Binary Hydrocarbon Mixtures for Modelling the Condensation Behavior of Natural Gas. Part I. The System Methane + Decane. *Fluid Phase Equilib.* **1992**, *71* (1−2), 143−168.

(52) Pauly, J.; Coutinho, J.; Daridon, J. L. High Pressure Phase Equilibria in Methane + Waxy Systems. 1. Methane + Heptadecane. *Fluid Phase Equilib.* **2007**, *255* (2), 193−199.

(53) Zamudio, M.; Schwarz, C. E.; Knoetze, J. H. Phase Equilibria of Branched Isomers of C10-Alcohols and C10 -Alkanes in Supercritical Ethane. *J. Supercrit. Fluids* **2011**, *58* (3), 330−342.

(54) De Goede, R.; Peters, C. J.; Van Der Kooi, H. J.; Lichtenthaler, R. N. Phase Equilibria in Binary Mixtures of Ethane and Hexadecane. *Fluid Phase Equilib.* **1989**, *50* (3), 305−314.

(55) Gregorowicz, J.; De Loos, T. W.; De Swaan Arons, J. The System Propane + Eicosane: P, T, and x Measurements in the Temperature Range 288−358 K. *J. Chem. Eng. Data* **1992**, *37* (3), 356−358.

(56) Peters, C. J.; Spiegelaar, J.; De Swaan Arons, J. Phase Equilibria in Binary Mixtures of Ethane + Docosane and Molar Volumes of Liquid Docosane. *Fluid Phase Equilib.* **1988**, *41* (3), 245−256.

(57) Gasem, K. A. M.; Bufkin, B. A.; Raff, A. M.; Robinson, R. L. Solubilities of Ethane in Heavy Normal Paraffins at Pressures to 7.8 MPa and Temperatures from 348 to 423 K. *J. Chem. Eng. Data* **1989**, *34* (2), 187−191.

(58) Kay, W. B.; Genco, J.; Fichtner, D. a. Vapor-Liquid Equilibrium Relations of Binary Systems Propane-n-Octane and Butane-n-Octane. *J. Chem. Eng. Data* **1974**, *19* (3), 275−280.

(59) Nieuwoudt, I. Vapor - Liquid Equilibria and Densities for the System Butane + Hexacontane. *J. Chem. Eng. Data* **1996**, *41*, 1024−1027.

(60) Hicks, C. P.; Young, C. L. The Gas-Liquid Critical Properties of Binary Mixtures. *Chem. Rev.* **1975**, *75* (2), 119−175.

(61) Joyce, P. C.; Gordon, J.; Thies, M. C. Vapor-Liquid Equilibria for the Hexane + Tetracosane and Hexane + Hexatriacontane Systems

DOI: 10.1021/acs.jced.8b01050
J. Chem. Eng. Data XXXX, XXX, XXX−XXX

at Elevated Temperatures and Pressures. *J. Chem. Eng. Data* **2000**, *45* (3), 424−427.

(62) Joyce, P. C.; Thies, M. C. Vapor - Liquid Equilibria for the Hexane + Hexadecane and Hexane + 1-Hexadecanol Systems at Elevated Temperatures and Pressures. *J. Chem. Eng. Data* **1998**, *43* (5), 819−822.

DOI: 10.1021/acs.jced.8b01050
J. Chem. Eng. Data XXXX, XXX, XXX−XXX